Development and Assessment of the Army Exoskeleton

A Major Qualifying Project Report
Submitted to the Faculty of the

WORCESTER POLYTECHNIC INSTITUTE

in partial fulfillment of the requirements for the
Degree of Bachelor of Science

in Mechanical and Materials Engineering, Biomedical Engineering, Robotics Engineering, and Computer Science

by

Liudmila Serebrennikova (BME, ME)
Alexander Strickland (RBE, CS)
Francesco Valagussa (ME)
Luke Reid (ME)
Nicholas Biliouris (RBE)
Roe Hendrick (ME)

Submitted: April 27th, 2023

Approved:

Dr. Mehul A. Bhatia (ME), Major Advisor

Dr. Songbai Ji (BME), Co-Advisor

Dr. Haichong K. Zhang (BME, RBE, CS), Co-Advisor

Keywords:

1: exoskeleton, 2: gait, 3:strain

Project ID: 17951

Acknowledgements

The authors of this paper would like to thank the following individuals for their assistance over the course of this project:

- Our advisors Professor Bhatia, Professor Ji, and Professor Zhang
- Christopher Nycz for his help with our motion capture study
- Maxon International Ltd. for their generous sponsorship
- Dosco Sheet Metal Manufacturing Inc.
- Barabara Furhman for her assistance in ordering parts
- Rodrigo Donascimento, and the WPI Washburn Shop

Table of Contents

Table of Figures

Abstract

The leading cause of injuries among US infantry were recognized to be the musculoskeletal traumas caused by the overuse of the lower body extremities. One of the possible solutions can be the use of advanced wearable devices that can reduce the amount of musculoskeletal strain in daily operations. An example of the such a device is an exoskeleton. In this project, our team has designed a lower body exoskeleton for use in military applications to reduce the fatigue of a soldier in their everyday challenges. The created exoskeleton contains support for the lower back, and it utilizes a combination of motors and sensors in a control loop to lower the amount of effort needed to carry a 70 lb load for ground combat troops.

Executive Summary

Introduction

An exoskeleton is a wearable device that enhances the physical abilities of the wearer by reducing the strain on their musculoskeletal system. In this paper, we will overview all the work that was done this year on this challenging and multidisciplinary project. Our group was tasked with creating a lower body exoskeleton for use in military applications that was designed to reduce the fatigue of a soldier in their everyday challenges. Through background research, goals were set for this project that allow the effectiveness of the design to be gauged and tested.

Literature Review

In order to provide in-depth understanding of the processes involved in the motion of walking, this section contains a detailed review on the muscle activity involved in the normal gait.

There is also a section that reviews exoskeletons that currently exist on the market for both military and non-military purposes. These products range from passive to active, using different materials and engines to perform effectively.Before any mechanical design implementations could be started, it was necessary to create a detailed plan for the electrical architecture of the future product.

Methodology

In order to understand the maximum torque that can be produced at the lower limb joints (left and right hip, left and right knee) during various activities, it was decided to perform the motion study using cameras, motion capture (MoCap) analysis software, and force plates. During the test, data was collected from three different types of movement (straight walking, walking stairs, and squatting). The male subject (6ft, 180lb) had performed all tests with and without additional weight on the shoulders (army rucksack that weighs 60 pounds). Captured data was rebuilt inside of the Vicon Nexus software and exported for further use in the design purposes.

The exoskeleton was supplied with four motors associated with four independent gearboxes, one at each hip and knee joint. The gearboxes were designed dependent on the Motion study capture torque values. In the final prototype, each individual gearbox contained a three-stage gear ratio

increase of 1:25.4 and was comprised of 44 individual components. All gearboxes could have been manually engaged or disengaged with a hand-operated clutch and were spring assisted. In case of a dead battery or an electrical issue with controls, operator use was enabled without motor assistance since, when disengaged, clutches were separated with wave springs.

The final iteration of the Computer-Aided Design (CAD) stage can be seen in Figure 28. Hip and knee joints of the exoskeleton were designed to act as pin joints providing a natural degree of flexion for both femur and tibia bones. The ankle joint was made as a series of simple compound pin joints at the back of the heel and sides of the ankle. This combination provided the full mobility of the foot (plantar and dorsiflexion, adduction and abduction).

The back support of the exoskeleton was redesigned to create a more robust part, while also considering user comfort and providing an area to mount the battery box. The safety mechanical stops were implemented as multi-purpose gearbox mounting plates.

The circuit for the exoskeleton project was designed using Altium Designer. The main components of the circuit included an emergency stop button, potentiometers for motor positioning, motors, motor controllers, a microcontroller, and a battery to power the motors. The specific microcontroller used was an Arduino Mega. The control loop had three main parts, checking the E-stop status, performing the calculations that were used to determine the current motor angle and the errors in the current angle to the desired angle, and lastly actually moving the motors. The motors were moved depending on their currently assigned direction. To ensure safety, maximum angles were set in the software, and all motors would be disabled if the current angle was somehow outside of the max angle range.

Manufacturing & Assembly

After the digital model of the exoskeleton was completed, it was necessary to manufacture the individual parts. The parts were manufactured using various manufacturing techniques, such as water jetting, milling, turning, 3-D printing, mill-turning and molding.

All simple in shape but structurally important parts were water jetted from A36 steel or 6061 Aluminum. For example, hydrocutter was used for a rapid and efficient manufacturing of the A36 steel plates used all over the developed exoskeleton.

For all the milling and turning operations, Autodesk Fusion 360® was used to produce NC code for each piece. The mill-turn technique was used for the mass manufacturing of the parts necessary in the clutch's activation. One of the more complicated pieces to manufacture were the clutches. In order to efficiently complete this operation it was made on the millturn, a machine that incorporates both the aspects of the lathe and the mill.

Small and non-bearing structures were 3D printed with Polylactic Acid (PLA) or Polyethylene terephthalate glycol (PETG) plastics with high infill levels.

The rest of the manufactured parts, complex in their shapes but with great structural integrity were made from resin-reinforced carbon fiber. In the final prototype, calf spline, heel cup, and foot base parts were manufactured using this technique.

Future Recommendations

From the creation of this exoskeleton, the main takeaways were recommendations on how to enhance the current design. There is a need to use stronger metals for the water-jet plates as well as for the clutches. This would allow for tear out to be minimized and eliminate the need of additional reinforcements. A recommendation for controls in this project is the use of kinematics in the gait cycle to calculate the acceleration of the end effector (in this case the foot) to tell how fast the person was walking. To effectively create a smart exoskeleton a higher bias on sensor input would allow for the exoskeleton to react to the users walk. Lastly, the use of brushless stepper motors would allow for better controls to be implemented to accurately read leg angles.

Conclusion

In conclusion, this project made significant steps as a first-round prototype. There are a couple more steps needed to make this exoskeleton a fully effective prototype, but overall, the group is very proud of the success made. We hope that a future group, building on our work, using these recommendations will create a truly smart and functioning army exoskeleton.

Introduction

According to the University of Pittsburgh Medical Center, a soldier's rucksack (backpack) weight should be in the range of 10% to 15% of the healthy body mass (UPMC HealthBeat, 2019). According to the report from the United States Department of the Army from 2021, the fighting load of the soldiers can be as high as 68.9 pounds (but should not exceed 100 pounds) and the approach march load can be up to 96.8 pounds (Department of Army Headquarters, 2021). According to the official United States Army website updated for 2022, the weight of male soldiers can fluctuate between 97 and 250 pounds with an average of 176.7 pounds. The weight of female soldiers can fluctuate from 91 to 236 pounds with an average of 160.8 pounds, depending on their height and age group (US Army Basic, 2016). Therefore, it means that the relative mass listed for an approach load can reach up to 54.7% of body mass for males and up to 60.2% of body mass for females. It means that the backpack load of US soldiers exceeds recommended values of 500% on average. At the same time, the average range of march for foot soldiers can be between 20 and 32 kilometers per day, while the velocity of the walk is determined by the average amount of load carried by the soldiers, but stays in the range of 2 to 3.5 kilometers per hour (Department of Army Headquarters, 2021).

One of the possible solutions to this problem might be an integration of robotics and mechatronic machines into the army routine. Exoskeletons or exosuits, are mechanical devices that allow individuals to improve their physical qualities (such as strength and endurance), thus reducing the incidence of musculoskeletal disorders (MSD) (Fox, S. 2019).

The goal of this project was to design, fabricate, assemble, and test an alternative, cost-effective lower-body exoskeleton for military applications. It was decided for the exoskeleton to use a combination of sensors, motors, and springs to augment the soldiers' abilities by reducing the strain on their musculoskeletal system.

The exoskeleton carries its own power supply and moves synchronously with the user. For an exoskeleton to be considered viable it must decrease the metabolic cost of movement i.e. a soldier that carries the weight of their gear and the exoskeleton should expend less energy than carrying just the gear (Marinov et al., 2019).

Literature Review

Biomechanics of Walking

The human musculoskeletal system converts chemical (food) energy into mechanical energy with maximal efficiency of roughly 25% (Laschowski et al., 2019). Therefore, it can be said that the human body has a low efficiency when it comes to the production of the energy necessary for the active movement of its own weight. From a biomechanical point of view, lower-body exoskeletons provide additional torque at the points of the flexion - hip, knee, and ankle joints.

Depending on the type of walking movement (i.e., slow/free/fast walk, run, jump, etc), different muscles are activated in the process of movement. There are five main groups of muscles responsible for the movement of the body: quadriceps, hamstrings, calf muscles, hip adductors, and gluteus muscles (Jackson, 2021). However, back muscles, abdomen muscles, and upper body muscles (to a degree) also play their role in the process of walking and balance support (Jackson, 2021).

Quadriceps are the most voluminous group of muscles in the body (includes five different muscles: rectus femoris, vastus intermedius, tensor of the vastus intermedius, vastus lateralis, and vastus medialis) located at the front of the thigh (Bordoni et al., 2022). Quadriceps are primarily responsible for hip (anterior) flexion, posture and balance maintenance, gait regulation. In addition, quadriceps aid in knee extension and stabilization of the patella (i.e. kneecap) to keep alignment over the femur (Bordoni et al., 2022; Biondi et al., 2021).

Hamstrings are a group of muscles located at the back of the thigh that includes three main muscles: biceps femoris, semimembranosus, and semitendinosus. These muscles are responsible for hip extension (posterior movement of the femur) and knee flexion (posterior movement of the tibia and fibula), as well as extending and rotating the hip joint (Rodgers et al., 2022).

Calf muscles are a group of muscles involved in the walking process. They are located above the heel to attach to the calcaneal tendon (i.e. the Achilles tendon) (Wong et al., 2021). It includes gastrocnemius, soleus (sometimes they are called one massive muscle with two sections), and plantaris (about 90% of people have this muscle) (Binstead et al., 2022). Providers call these three muscles the triceps surae (Wong et al., 2021). This group of muscles provides support during standing

and enables lower leg and foot movement during motion (walk or run) propulsion. It also allows jumping, rotation of the ankle, flexion of the foot, and “locking” of the knee (Binstead et al., 2022).

The muscles in the medial compartment of the thigh are collectively known as the hip adductors (Jeno et al., 2021). This group of muscles usually extends from the pelvis to the femur bone and includes adductor longus, adductor brevis, adductor magnus (consists of adductor and hamstring portions), and gracillis (Jeno et al., 2021). In closed-chain activation, adductor and hamstring portions of adductor magnus help stabilize the pelvis and lower extremity during the stance phase of gait and assist in postural control (Benn et al., 2018). Along with adduction, the adductor part of the adductor magnus also flexes the thigh, whereas the hamstring portion adducts but extends the thigh (Benn et al., 2018). They also have secondary roles including hip flexion and rotation (Jeno et al., 2021).

Gluteus muscles involve three main muscles: gluteus maximus, gluteus medius, and minimus. The gluteus maximus' primary function is to externally rotate and stretch the thigh (Elzanie et al., 2022). Despite being a powerful extensor, gluteus maximus only acts during a specific sort of movement (such as rising from sitting, straightening from a bending position, walking upstairs or on a hill, and running) (Elzanie et al., 2022). Additionally, it supports the trunk and the pelvis, which is crucial when someone is standing on one leg. The gluteus maximus stabilizes the femur by joining with the tensor fascia lata (Kim et al., 2015). The gluteus medius and minimus, located deeper in the hip, both work from the pelvis to abduct and rotate the thigh internally (Shah et al., 2022). Gluteus medius serves as the primary hip abductor and acts from the femur to stabilize the pelvis and maintain the trunk upright when standing on one leg, running, and walking when one leg is off the ground (Shah et al., 2022). Gluteus minimus is the smallest muscle in the gluteus muscles complex and works synchronously with the gluteus medius to abduct and stabilize the hip during movements that require balance (Greco et al., 2022).

Muscles enable walking by providing vertical support and allowing forward movement. The body's mass center experiences periodic vertical and fore-aft accelerations when moving normally. These accelerations are proportional to the ground reaction force. Muscles help create a vertical ground reaction force greater than body weight during early stance, which causes the body mass center to rise faster. The ground response force is less than body weight during midstance, which

causes the body mass center to accelerate downward. During a late stance, muscles contribute to a vertical ground response force larger than body weight, accelerating the body mass center upward (Liu et al., 2005).

Exoskeletons on the Market

Currently, the open market has a wide variety of alternative models of exoskeletons for a diverse range of applications: medical, rehabilitation, commercial, and military. This section will focus on the creation of exoskeletons targeted for use in the military. The first and largest suit is the Raytheon XOS-2, which uses “high-pressure hydraulics to allow the wearer to lift heavy objects at a ratio of 17:1 (Krishna, 2020)”. This means that what the user feels as 1 lb, is in reality a 17 lb load. The XOS-2 is a large improvement from the first iteration, the XOS-1, is much more energy efficient. The exoskeleton itself weighs about 95 kg which is a lot more than most other suits, this is due to its large size and the fact that it enhances both the lower and upper body. The suit is powered by an internal combustion hydraulics engine with electrical systems, but a big downside is that it must remain tethered for power (Krishna,2020).

Figure 1:XOS-2 Exoskeleton (Raytheon Xos-2 Exoskeleton, 2020)

A second suit that is being developed for use in the army is the Onyx, created by Lockheed Martin. The Onyx is a much smaller exoskeleton, resembling more of a knee brace that covers the entire leg. It works by using predictive artificial intelligence that is integrated at the feet, knees, and hips to collect data and predict the users' movements. This allows the motors to provide the correct amount of torque to support the user in his actions (Watson, 2020). The advantage of this suit is that it allows users to be able to do repetitive motions that they are already capable of, but with less strain on their musculoskeletal system. It is focused on knee-intensive activities such as climbing and descending stairs and hills. Unlike the XOS-2, it is not a sort of "iron man" suit that gives the human super strength, but it is a much more applicable design that could be given to soldiers across the globe. Weighing only 20 pounds including its battery, the Onyx is a much more portable and feasible design for use in the military. To maintain such a low weight, the system is made of "carbon fiber, aluminum, plastic, fabric, and a bit of titanium" (Watson, 2020). Since it is so small and lightweight, it can be transported easily. Not only is it useful for riflemen and artillerymen, Lockheed Martin program manager Keith Maxwell says it can also be useful for combat medics who carry their equipment around the battlefield and need to remain active throughout the day. Another major advantage of the suit is that it contains eight hours of battery life. This allows soldiers to go on long expeditions throughout the day without having to recharge their suits. Overall the Onyx not only helps with fatigue reduction in the present, but also helps long term joint health if worn for extended periods of time.

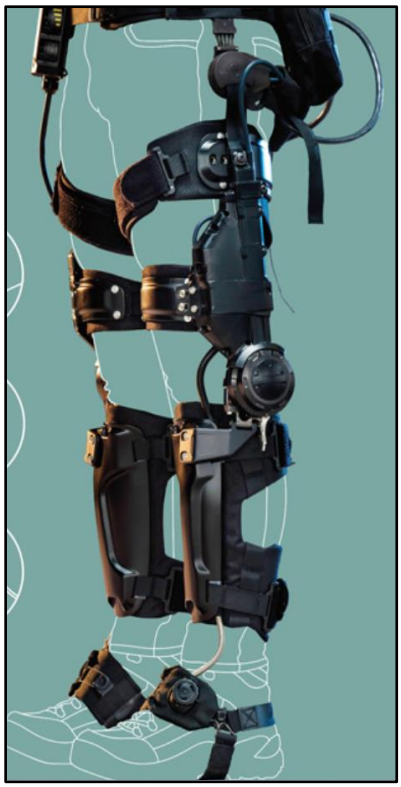

Figure 2: Onyx Exoskeleton (Watson, 2019)

A third suit that is very different from the first two is the Mawashi Uprise Tactical Exoskeleton. This suit is a “wearable device that redirects the load carried by soldiers to the ground through mechanical levers” (Mawashi, 2020). The major difference is that this suit is passive, meaning it requires no power and works through ergonomics. Mawashi’s main goal has been to decrease musculoskeletal injuries to soldiers, often caused by carrying heavy weights such as backpacks for a long period of time. The lightweight suit is made of titanium and is very effective at preventing these injuries while still giving the soldier a full range of motion. The Uprise can transfer up to 50-80% of a soldier's load onto the ground, drastically reducing the fatigue on their body. This could be a major breakthrough for the military as it has been proven that fatigue “reduces the efficiency of the soldier in a hostile environment” (Mawashi, 2020). This could mean the difference between life and death for many soldiers as they fight on the front lines.

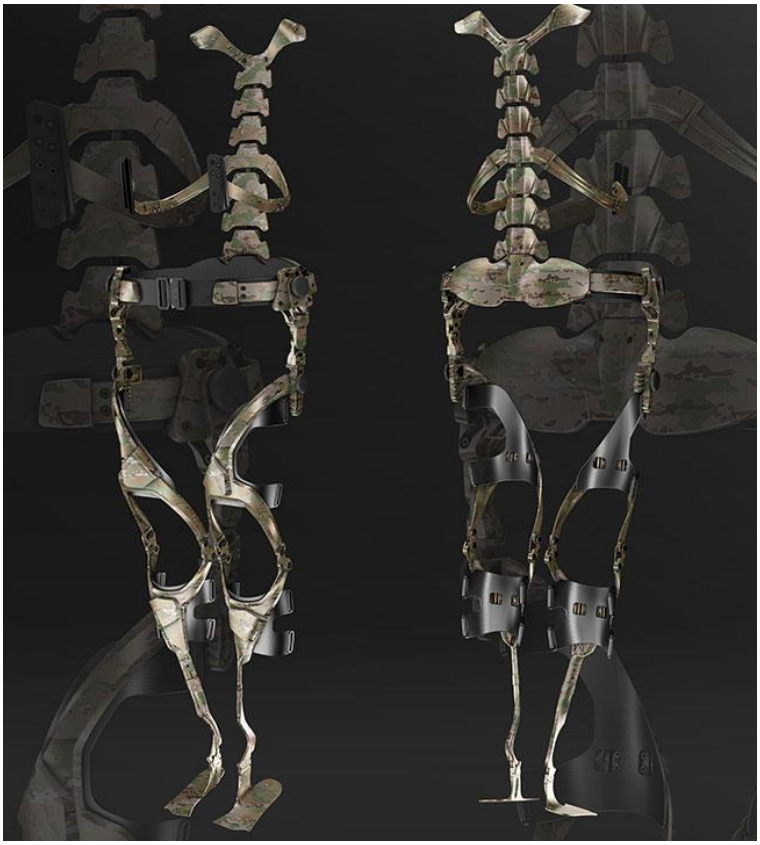

Figure 3:Mawashi Uprise Tactical Exoskeleton (UPRISE Passive Load-Bearing Exoskeleton)

Non-Military Applications of Exoskeletons

The application for exoskeletons is not only on the front lines but also for industrial use on the assembly lines. A company called SuitX has been developing multiple suits that support the users' legs, back, and shoulders throughout the workday as they complete repetitive strenuous tasks in awkward positions. The LegX weighs a light 10 pounds and reduces the user's body weight load by 30 to 50 percent. It uses a battery boost along with springs and clutches to support the knees, and in the lock mode, it is able to lock out at certain angles to imitate a seat that extremely diminishes the strain on the user's legs while squatting. It also has a smart mode that has an application similar to the onyx, reducing the weight of the user while walking or going up and down stairs, transferring part of the user's weight into the ground.

It is not only companies coming up with innovative technologies for exoskeletons, as many researchers are also trying to come up with new solutions. The PALexo is an exoskeleton that uses Gas springs, which is a cylinder with compressed gas and a piston. Two of these are used for each leg

in their design, trying to maximize the weight that can be lifted by the user. Their goal is to “provide large force in the direction of elongation and in the standing phase, but they need only provide little force in the direction of shortening in the swinging phase” (Wang, 2022). This will be a major focus of the smart exoskeleton as well, attempting to gauge when the user needs the motors to be activated, and when the user needs them suppressed. The PALExo ran into a problem while using series-parallel elastic actuators, finding that they were great at increasing the torque, but their bulkiness impeded the user's performance (Wang, 2022).

Military Applications for Exoskeletons

There are a lot of tasks in the military that could be helped and improved with the use of a well-developed exoskeleton. Almost everything falls under one of these categories including lifting and carrying heavy weight, improved movement, and maneuverability, or specific combat tasks. The military services have previously demonstrated interest in advanced human-integrated technologies, like exoskeletons, by the release of related design. In a contract for exoskeletons posted by the department of defense (SAM.gov, 2022), they specified certain tasks of interest and were looking for vendors to apply.

One military application of an exoskeleton would be for a unit supply specialist (92Y) in the army. They are required to organize supplies on a military base and carry up to 100lbs and 50lbs on a consistent basis. They are required to receive, inspect, inventory, load/unload, store, issue and deliver supplies and equipment. This would be perfect application for an exoskeleton because it does not require complex athletic movements, but rather can be used to reduce strain from redundant movements from lifting heavy loads on soldiers in this occupation (92Y Unit Supply Specialist, n.d.).

Another possible application for this exoskeleton could be for a member of infantry (11B) in the army. An individual in this position would need to occasionally carry 100lbs and frequent lifting of 50lbs. They are required to perform as a member of a fire team during drills and combat, as well as aid in the mobilization of vehicles, troops, and weaponry. This occupation also requires maintenance and storage of weapons and munitions. This occupation requires a lot of movement as well as heavy

lifting which will be perfect for the application of a lower body exoskeleton. It allows the upper body to remain free to turn and manipulate a weapon during combat while supporting the legs in the constant lifting and troop movement (11B Infantryman, n.d.).

Even though the contract from the DOD mentioned earlier has since expired there is still broad sponsorship from the military that an exoskeleton falls under. Under the future warrior technology integration category they mention interests in soldier mobility and load assistance solutions. An exoskeleton designed with load-bearing back support would be a good solution to assist with carrying a heavy backpack with less fatigue**.**

Interview with Active Military

After speaking with a member of the active military we were able to get many questions answered that will help us to better design this exoskeleton. A typical military rucksack weighs between 60 - 80 pounds. A specific procedure is used to pick up a rucksack to minimize the risk of injury to the wearer. This involves picking it up upside down over the head and letting the straps fall onto the shoulders. The most common long term injuries in the military involve the neck and back from carrying constant load.

One of the tasks an exoskeleton would be most useful for is logistics. Enabling someone to carry a load that would otherwise require a second person or external equipment. It is very important that the exoskeleton is comfortable and more useful to the user than a hassle. It could actually hinder the user if it just adds to what the soldier needs to carry and therefore slow them down. It should also be compact and light enough to be carried by one person and put on alone. An ideal runtime for such an exoskeleton would be at least four hours and be able to recharge in the same amount of time. Overall the military member we interviewed believed an exoskeleton could be great but it needs to be focused towards logistics and not combat**.**

Review of Autonomous Exoskeleton for Paraplegic Assistance

Last year, a group of four fourth-year mechanical engineering students and one fourth-year biomedical engineering student at Worcester Polytechnic Institute, compiled a report on their design,

fabrication, and verification of a cost-effective exoskeleton “capable of lifting a 200 lb human and supporting the motions of walking, sitting, and standing (Waterman et al., 2022)”.

The six objectives of their exoskeleton were: the exoskeleton must be able to support the motions and forces of (1) standing, (2) sitting, and (3) walking. (4) Ensuring that the exoskeleton has a reasonable cost, (5) must be safe to use, and (6) must be easy to put on and operate. Using these objectives as a guide, they decided on a single piece assembly using a joystick for user control of the exoskeleton. Using the information collected during expert interviews, they created a client statement to guide their project: “the objective of this project is to design and build an individualized lower limb exoskeleton to assist paraplegic individuals in standing and walking that costs less than $10,000 to produce (Waterman et al., 2022)”.

The final design of the exoskeleton is comprised of a frame with four total motors. There is one motor at each hip and knee joint with gearboxes on each to increase torque, a battery/electronics pack at the back of the hips, springs at the ankle to control degrees of freedom, and straps at the thighs and calves to hold the lower extremities. The final design of the hardware includes a 48 volt power supply, two microcontrollers, a pulse oximeter, an emergency stop button, several relays, motor speed controllers, and other smaller components. The software design uses timer-based interrupts to constantly measure data from the joystick, motor positions, and safety sensors. The motor position is controlled using case statements by changing the motor speed of each joint based on its real-time angle. The data used in the case statement was collected using motion capture data of one of the group members walking with crutches (Waterman et al., 2022).

Every component of hardware and software was extensively tested before a human subject was allowed to get in the exoskeleton. The full exoskeleton with a human participant was tested in the apartment style PracticePoint Lab at Worcester Polytechnic Institute. This lab has a harness running around the apartment allowing all types of movement to be tested while the user is supported by the harness in the case of failure. The motions of sitting, standing, walking, turning left, and turning right were tested successfully.

Exoskeletons currently on the market/in development are cost-prohibitive to purchase due to their high cost and poor coverage from insurance. Once constructed, the exoskeleton was able to

support all of the relevant motions laid out. The user was able to successfully sit up, walk forward, turn left, walk forward, turn right, and sit down. The user, also a member of the student group, described using the exoskeleton as “Pretty different from walking normally, but definitely possible with some practice (Waterman et al., 2022)”.

In conclusion, the team was able to meet all six of the original objectives. The first three objectives were confirmed during the user testing at PracticePoint when the team member performed the motions of walking, sitting, and standing and the exoskeleton supported their weight and did not sustain damage. The fourth objective was confirmed during a cost analysis where it was determined that the total cost of the production of the exoskeleton was $10,080, substantially less than current devices on the market. The fifth objective was met during the user testing when the user reported no adverse effects of the device. Finally, the sixth objective, the exoskeleton must be user friendly, was confirmed during user testing when the user described putting on and taking off the device as “Fairly easy to remove. The supports are pretty comfortable”. The team was constrained by the budget and one-year deadlines so there is further work that can be done by future MQP teams. Overall, the Autonomous Exoskeleton for Paraplegic Assistance was a success and met all of the objectives laid out at the beginning of the project (Waterman et al., 2022).

Power Options

Choosing whether the exoskeleton would be tethered or battery-powered was a very important decision that would greatly affect how the project would move forward. Looking at what's on the market gave good insight into the pros and cons of both options. Tethered can be much better for physical support and allow for much greater power needs but has extremely low mobility. Battery-powered needs to be self-supporting and has limited energy capacity but can go anywhere. Since the exoskeleton is being designed for military use, good mobility is a top priority. Given this, the exoskeleton will need to be battery-powered.

There are many types of batteries to choose from on the market. Three kinds that were researched included Nickel-Cadmium (NiCd), Nickel-Metal Hydride (NiMH), and Lithium Ion (Li-

ion). These three were researched because they are all rechargeable and prominent on the market. Important factors when choosing battery type include charging capacity, energy density, and life cycle.

Nickel-Cadmium batteries are now an older technology but are relatively cheap. They have a life cycle of about 1000 recharges before they reach approximately 80% of their maximum capacity (Battery Cell Comparison, n.d.). A major downside to NiCd is they need to be fully discharged before recharging again. If not they will degrade extremely fast and won't reach their full life cycle. This type of battery also has relatively low voltage compared to other options.

Nickel-Metal Hydride batteries have essentially replaced NiCd batteries but they are much more expensive. Both have about the same life cycle but NiMH batteries can be partially discharged and recharged without degrading (Rechargeable Batteries Guide, n.d.). NiMH batteries also have a much larger capacity because they have a much higher energy density.

Lithium Ion batteries have a much higher energy density than both of the other options researched. This makes them the best option for use in the exoskeleton for optimal mobility. Li-ion batteries can also deliver about triple the voltage of NiCd and NiMH batteries (Lithium-Ion Battery, 2020). They will also not degrade over time from partial discharge and recharging. A down side of Li-ion batteries is that they are significantly more expensive than the other types, about 40% more than Ni-Cd.

Encoders

Motors can be outfitted with encoders, which are data points built into the motor which relay the exact positional data of the motor in relation to the zero-position of the motor. By reading the encoders of a motor, you can tell where the motor is turned to, when it went there with respect to time, and with time and location you can determine speed, acceleration, as well as many other figures relating to motor performance (Anderson, 2019).

Encoders are largely broken into two types of encoders: Incremental and absolute. Of these two types, encoders can then be rotary encoders or linear encoders. Linear encoders act in a straight

system, whereas rotary encoders are essential in rotational positional data. Absolute encoders work in a way such that each time there is a rotation along the encoder, the signal from the encoder is a direct positional piece of data that is the exact location of the turn. In contrast, the incremental encoder uses the current positional data vs the time it was last moved, meaning that it is only receiving data every time the encoder is shifted in a certain way (Dynapar, 2022). For the application of the military exoskeleton, we will want to utilize the absolute encoder, so that the current positional data is always being reported and we can tell when there is any rotation.

The Maxon EC90 Flat Brushless motor that we will be using in this project has multiple encoder channels. The motor has binary encoders of up to 4096 impulses per turn, as well as a higher resolution available which offers up to 6400 impulses per turn (Maxon, 2022). The higher impulse count can give us a more accurate read of the motor position, as well as factor in the rest of the data that we might want at a certain time, such as acceleration, speed, and velocity.

Sensors

In order to accomplish the tasks of commanding the motors at proper time, the exoskeleton most importantly needs to know when and when not to move. If not accomplished by the encoder counts on the motor measuring acceleration, then this will have to be accomplished by reading live sensor data to do the same thing.

Force Sensors

In terms of sensor, the choice of a force sensor is important in order to figure out when to actuate motors. The force sensor will ideally act as a way to sense a threshold that when a certain force is detected, actuate the motors.

For force sensors, there are multiple types including strain gauge sensors, load cells, and force sensing resistors (Thomasnet, 2022). Strain gauges are going to be most beneficial for this project. Strain gauge resistors have a varied output based on the amount of force that is applied to a resistor located on the sensor. The more pressure applied to the sensor, the more the resistance increases, thus

allowing us to read the amount of force being applied to it across the area of the sensor. This can be translated to Newtons, and then allow us to determine a threshold of force detected before actuating the motors.

Proximity Sensors

Proximity sensors are ideal if the force sensor proves to be unreliable. Using a proximity sensor, we can tell the exact speed that a joint is moving with respect to time. “A proximity sensor uses an electromagnetic field to measure changes in the distance to an object. As a gear moves past the sensor, it measures a variation in distance; close (tooth) and far (notch). The rotation speed can be determined based on the time between these events.” (Hemmes, K., & Bakker, 2019) Using the information provided by a proximity sensor, we can tell how fast a gear is moving and tell how much force to apply based on the movement of the gear.

The proximity sensor’s data provides positional, as well as time data so that we can determine even where to add more torque, and works in relation to the use of motor encoders to be able to program certain thresholds that will need more and less torque.

Electrical Impulse Sensors

Another approach that we thought of for detecting movement was reading the electrical pulses of the body from certain muscles with respect to actuation. If a certain amount of electricity is detected from a muscle located on the leg, for instance, we could actuate the motor accordingly, thus driving the leg forward. Something like the MyoWare 2.0 Muscle Sensor would be used, which reads the electrical output of each muscle to determine how much it is being used (SparkFun, 2020).

The way that the sensor works, the more the muscle is flexed, the higher the output unit is of the sensor. If we attach electrical sensing pads to the sensor, and have it communicate with the microcontroller, we can tell where the subject is using the most muscle force, when they are, and how much to actuate the motors in order to alleviate stress from the subject. This would be slightly

challenging due to the delay of the readings, but would provide a highly accurate reading of the muscle, and provide accurate data to the microcontroller.

Conclusion of Literature Review

This literature review provides a comprehensive analysis of the available sources that might be relevant to the process of the design, fabrication, and assembly of a lower-body exoskeleton. Each of the team members summarized the information from the open sources that was relevant to their area of the design respectively.

Therefore, currently we have sections dedicated to the available basic available information ("Biomechanics of Walking", "Exoskeletons on the Market", etc), "NABC" analysis ("Military Applications for Exoskeletons", etc), and the hardware parts of the projects (sections about motors, sensors, etc).

Taking into account the biomechanics of the movement, our design should be balanced in terms of equally taking the load from quadriceps, hamstrings, calf muscles, hip adductors, and gluteus muscles. At the same time, we should consider the minimal constraints to the degrees of freedom of key joints since this can cause a significant loss in balance while walking.

When it comes to the military exoskeletons on the market, the Onyx design is the most feasible starting point for this project given the time and funding. Its use of motors and its lightweight properties make it very useful in the military field. The Mawashi exoskeleton could also be used as a good base to see how weight is distributed from the soldier's backpack to the ground.

Last year's Major Qualifying Project team layed significant groundwork this project intends to build on. Although the application of the exoskeleton is transitioning from paraplegic to military, many of the objectives and verification methods the team used will be maintained in this year's adaptation.

Researching and choosing the correct power source is crucial to the success of this project. Picking the option that maximizes the runtime of the suit while still being compact and light enough

to allow full mobility of the user will be essential. Based on this criteria, Lithium-Ion batteries will be the most feasible option for the exoskeleton.

The current exoskeleton needs an enhanced and advanced sensor setup in order to actively aid the human gait cycle. The current iteration of the exoskeleton lacks a power supply with enough current to fulfill the needs of all four motors, and will thus need a new power system. We will attain a power supply that will adequately power all four motors, and design and allocate a sensor system with the proper ability to aid in the execution of the human gait cycle.

Methodology

Motion Study

In order to understand the maximum torque that can be produced at the lower limb joints (left and right hip, left and right knee) during various activities, it was decided to perform the motion study using cameras, motion capture (MoCap) analysis software, and force plates.

Initially, primitive motion was performed. That study involved AMTI force plates, light-reflecting stickers, and the camera. From the captured video it was possible to determine joint angles at various stages of the normal gait cycle via manual mocap software. This information was then used to calculate the approximate torque during straight walking. However, it was decided that the capabilities of the available equipment were very limited. Therefore, the team made a solution to expand the existing dataset with additional motion studies with more advanced automatic technologies that were provided by the Practice Point Motion Capture Laboratory (PP MoCap Lab), run by Professor Gregory Fischer. Equipment used in the PP MoCap Lab included AMTI force plates, Vicon Nexus Analysis Software, 12 MoCap cameras, and light-reflecting markers.The methodology below describes the use of the Practice Point Motion Capture Lab equipment.

Testing Procedure

It was decided that all the tests would be performed on the single participant that will work as our test patient for this exoskeleton.

After the MoCap cameras and force plates were calibrated and prepared for the test, 16 reflecting markers were placed according to the “Vicon Plug-in Gain Reference” manual, i.e. on the Right and Left Anterior Superior Iliac, Right, and Left Posterior Superior Iliac, Right and Left Thigh, Right and Left Knee, Right and Left Tibia, Right and Left Ankle, Right and Left Toe, and Right and Left Heel.

During the test, data was collected from three different types of movement (straight walking, walking stairs, and squatting). The male subject (6ft, 180lb) had performed all tests with and without additional weight on the shoulders (army rucksack that weighs 60 pounds).

After the trial runs were over, the captured data was rebuilt inside of the Vicon Nexus software and all reflective markers were identified in order to run a Plug-in Gait Analysis.

Results and Data

Collected and analyzed results were exported in the Excel spreadsheet format.

Figure 4: Knee moments in squat motion around the x-, y-, and z-axis, respectively.

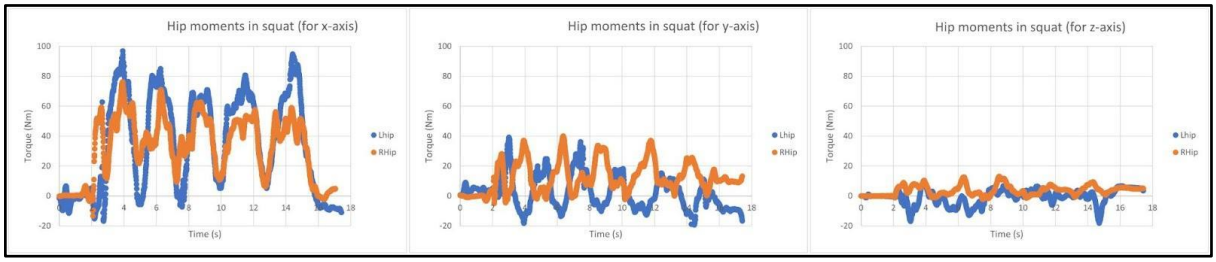

Figure 5: Hip moments in squat motion around the x-, y-, and z-axis, respectively.

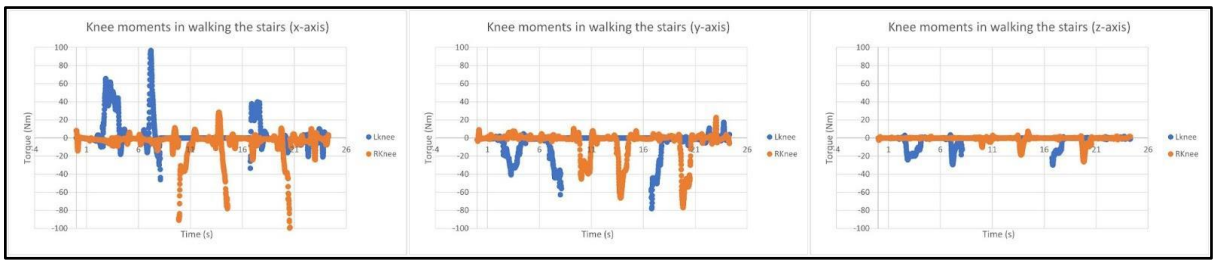

Figure 6: Knee moments in stair walking motion around the x-, y-, and z-axis, respectively

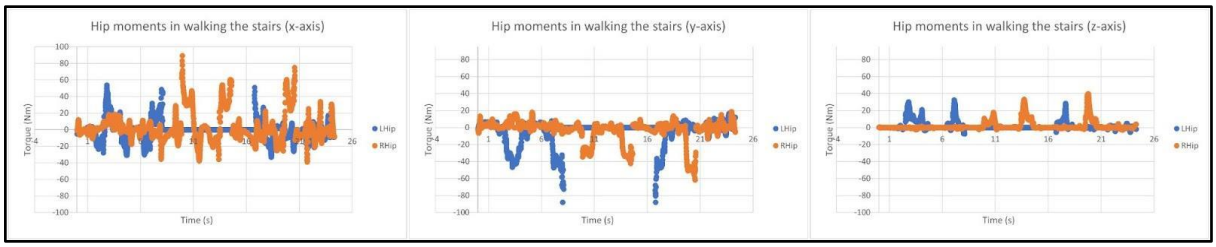

Figure 7: Hip moments in stair walking motion around the x-, y-, and z-axis, respectively.

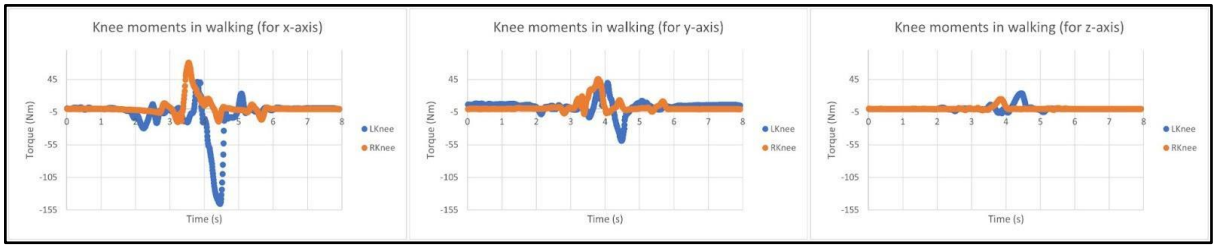

Figure 8: Knee moments in walking motion around the x-, y-, and z-axis, respectively

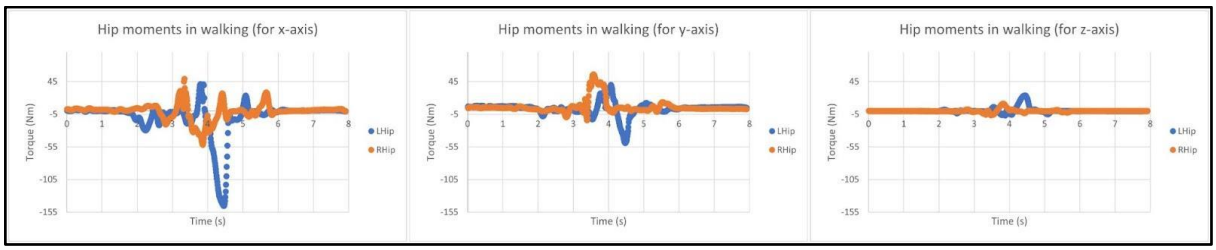

Figure 9: Knee moments in walking motion around the x-, y-, and z-axis, respectively

Results Application

Data from the performed motion study was used to estimate the maximum torque that can be expected as the system output power. According to the data presented in the Results section of the Motion Study chapter, the maximum torque at the knee happened when the participant was walking up the stairs and was equal to ~96 Nm. Maximum torque at the hip was achieved by doing basic squats, the values have reached up to ~ 100 Nm. For simplification purposes, it was concluded that the output of the any gearbox design should be close to 100 Nm.

Mobility of the Joints

Hip Joint

In order to avoid the restriction of leg mobility, it was decided that a mechanical joint that connects the pelvis-supporting construction and bar that follows along the femur bone would be presented in the two mechanisms. The combination of two would make it possible to perform the motion in two planes - lateral/medial and ventral/dorsal. In order to keep the flexibility in the ventral/dorsal plane but provide the limb with additional torque, it was decided to use the motor-driven shaft/bearing. However, the power of motion in lateral/medial planes is less necessary,

therefore, it was decided that the pin-hinge, that makes this motion possible, would be undriven. Here and later this mechanical joint would be called “hip joint”.

Knee Joint

In order to facilitate the mechanical task that was assigned, it was decided to simplify the level of mobility of the knee joint and characterize its motion as a rotation around the knee (where knee joint acts as an origin). Therefore, the mechanical joint that connects the bar following along the femur bone and the tibia would be presented as the shaft/bearing. This mechanical joint is also motor driven. Here and later knee mechanical joint would be called “knee joint”.

Ankle Joint

For the stability of gait, it is important to save the mobility of the foot and ankle. Therefore, it was decided that the joint that connects the bar following along the tibia and foot “stirrup” (here and further called “ankle joint”) would be presented in the undriven shaft/bearing.

Design and Computer-aided Design (CAD) Iterations

CAD Iteration I

At the first design iteration, it was decided to create an intelligible mechanical structure that would integrate all of our final goals in the simplest form. It can be seen in Figure 4. The full mobility of the foot (plantar and dorsiflexion, adduction and abduction) was provided with simple pin joints at the back of the heel and sides of the ankle. Similar pin joint at the knee area was added to provide a natural degree of knee flexion (flexion, extension). In order to encompass the natural behavior of the hip ball-joint, a developed exoskeleton joint was made as a combination of two pin joints that disable both lateral-medial and anterior-posterior hip motion (abduction and adduction, flexion and extension). For the lower back, a double hinge joint was added so that the exoskeleton user could bend over, while also incorporating a second joint that is higher up to allow the extra- and intra-rotation of the hip.

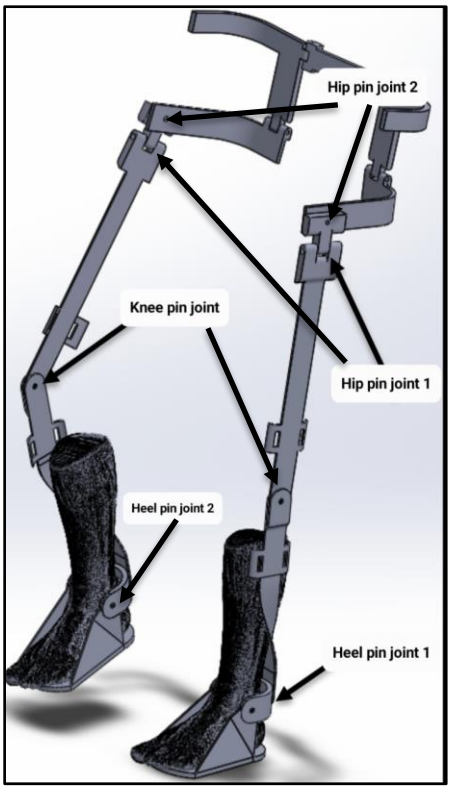

Figure 10: Early CAD design.

CAD Iteration II

In the second design iteration, it was decided to focus on the work of the exoskeleton hip joint (Figure 12). The lower back support piece was replaced with one solid band that wrapped around the lower back to the hips. The joints providing external hip rotation were moved closer to the wearer's hip joint to avoid user discomfort.

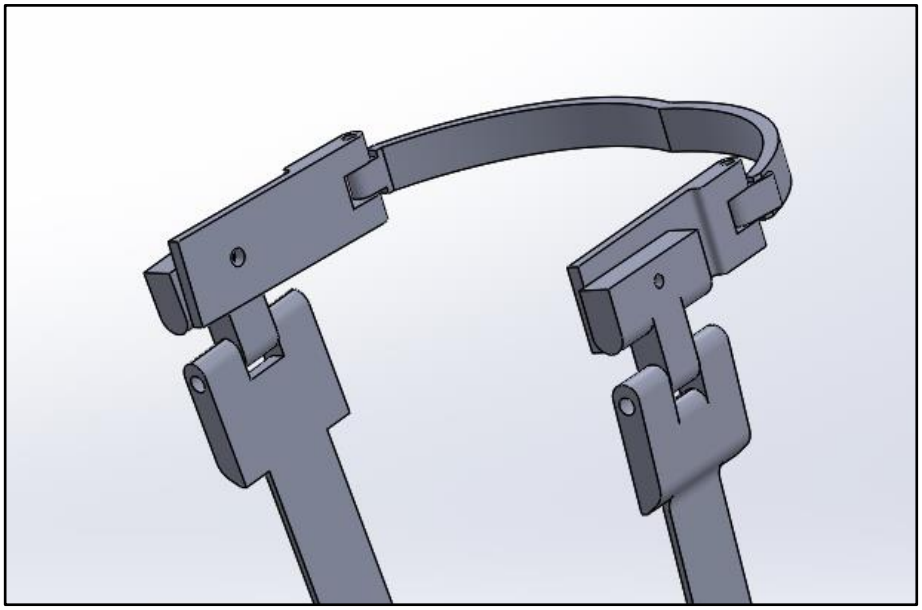

Figure 11: New Lower Back Design

In an attempt to improve on the design of the Autonomous Exoskeleton for the Paraplegic Assistance (Hersum et. al., 2022), a couple of different gearbox designs were investigated to identify a more compact version. On the example of the knee gearbox, two different approaches to the gearbox construction design were implemented. The initial gearbox design was based off last year's gearbox model but was improved by removal of all excess material on the mounting plate. Similarly, to the last year's model, this gearbox had a 100:1 gear ratio. On the other hand, planetary gearbox design was found to be the optimal approach for creation of a high torque output while staying compact. However, all the up-to-specification market gearboxes were found to be outside of our budget limits. Therefore, it was decided to move forward with the first option. Figure 6 demonstrates the two of the developed designs, where the initial gearbox design is demonstrated on the left and planetary gearbox is shown on the right. An initial version of knee mechanical stops was added to this iteration.

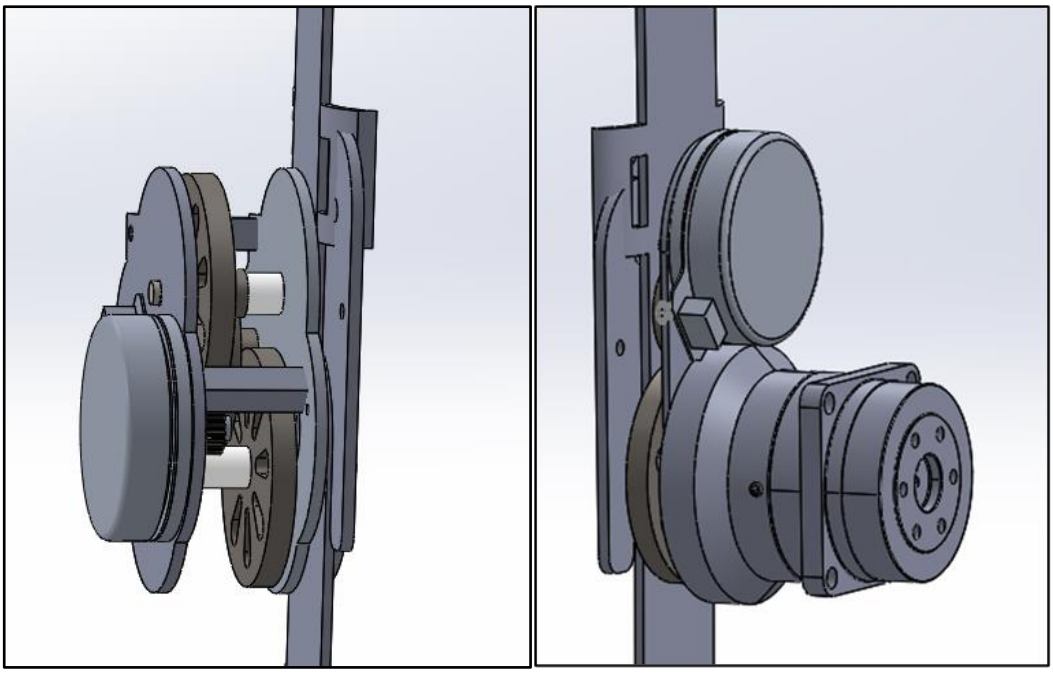

Figure 12: Initial Gearbox Design on the left and Planetary Gearbox on the right

CAD Iteration III

Therefore, in the third design iteration, the mechanical stops were altered to fit the developed model correctly (Figure 14). The mechanical stops at the knee were designed to prevent the knee extension (forward motion) past 180 degrees along with stopping knee flexion (back motion) past 90 degrees.

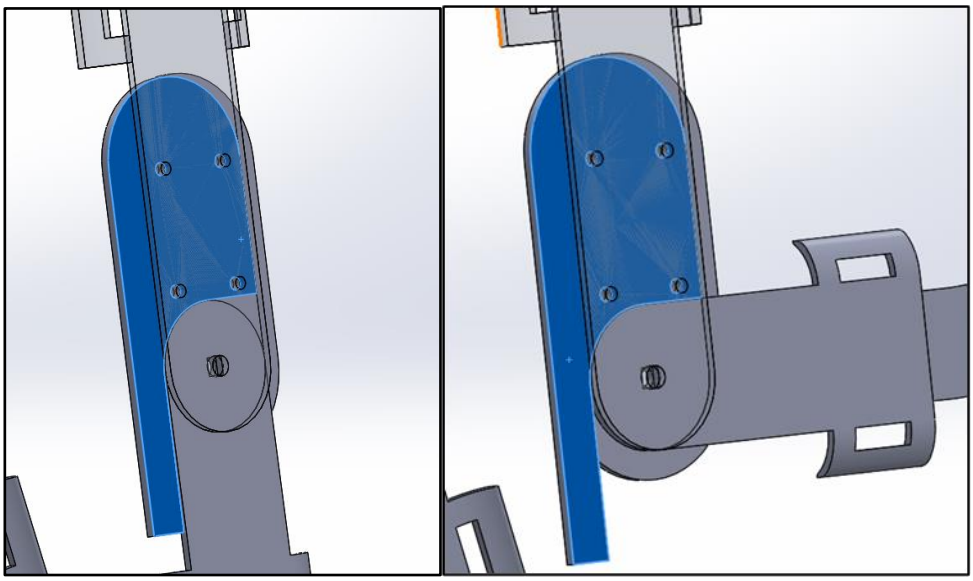

Figure 13: Knee bent at 180 degree stop and Knee bent at 90 degree stop. Stops are highlighted in blue.

The second pair of mechanical stops were added at the exoskeleton hips. The developed design was preventing the femur extension (back motion) over 45 degrees and flexion (forward motion) over 90 degrees.

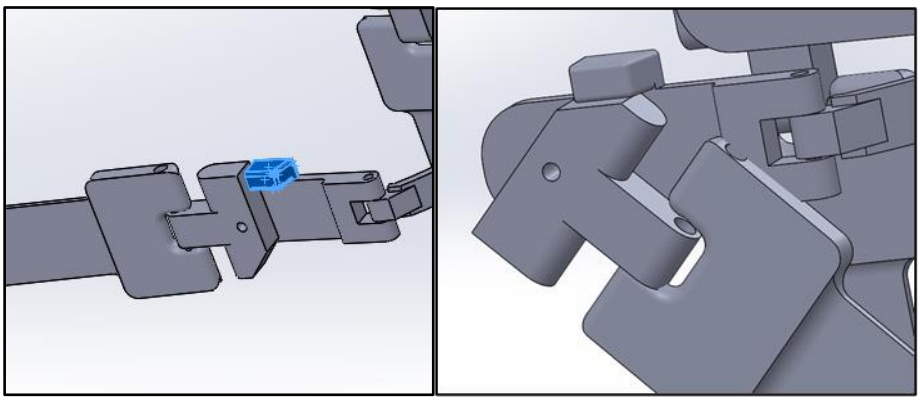

Figure 14: Leg rotated 90 degrees forward to stop and Leg rotated 45 degrees backwards to stop.

CAD Iteration IV

The focus of the fourth iteration was the addition of fasteners. Standard industry fasteners (screws, bolts, shafts and bearings) from McMaster-Carr® were chosen and implemented to hold the desirable weight of each joint.

At the same time, it was attempted to make the frame of the exoskeleton lightweight and manufacturable. The mass of the major frame was reduced by removal of the metal from the areas of

the low stress. In case of this project, cutouts were implemented along the Femur plate (Figure 16). On top of that, the described bar was divided into two parts (flat plate with triangular holes and connective piece to attach this bar to the lower back segment) to increase manufacturability (Figure 17).

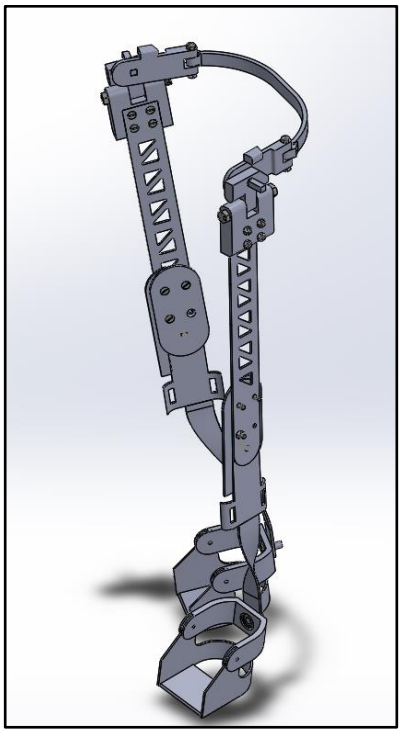

Figure 15: Full-height design developed in the fourth CAD iteration.

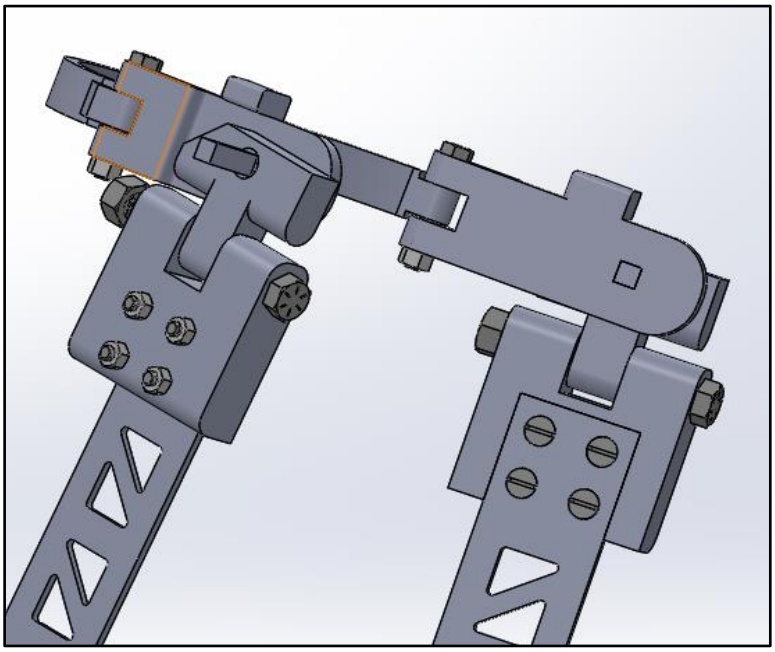

Figure 16: Hip joint design developed in the fourth CAD iteration.

CAD Iteration V

The fifth iteration was concentrated on the completion of the exoskeleton joints at the hip and ankle areas. After some consideration, it was concluded that the use of the D-shaped rotary shaft to attach the legs of the exoskeleton to its hip piece (Figure 18) would resolve a couple of acute problems. First, with the use of a high strength bearing, D-shaped rotary shaft allows hip rotational motion with minimal friction. Second, the use of the D-shaped shaft simplifies the following manufacturing and assembling processes.

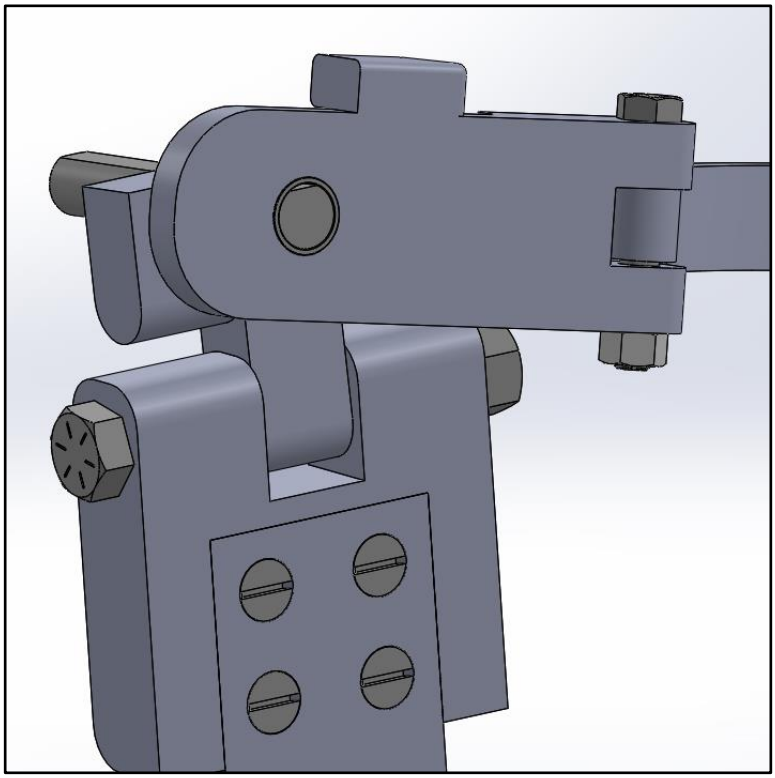

Figure 17: Hip joint design developed in the fifth CAD iteration.

On top of that, bearings were added on the outside of ankle joint and on the back of the heel of the exoskeleton. Since the back of the heel is a high stress area, the bearings were supplemented with bolts to secure the ankle.

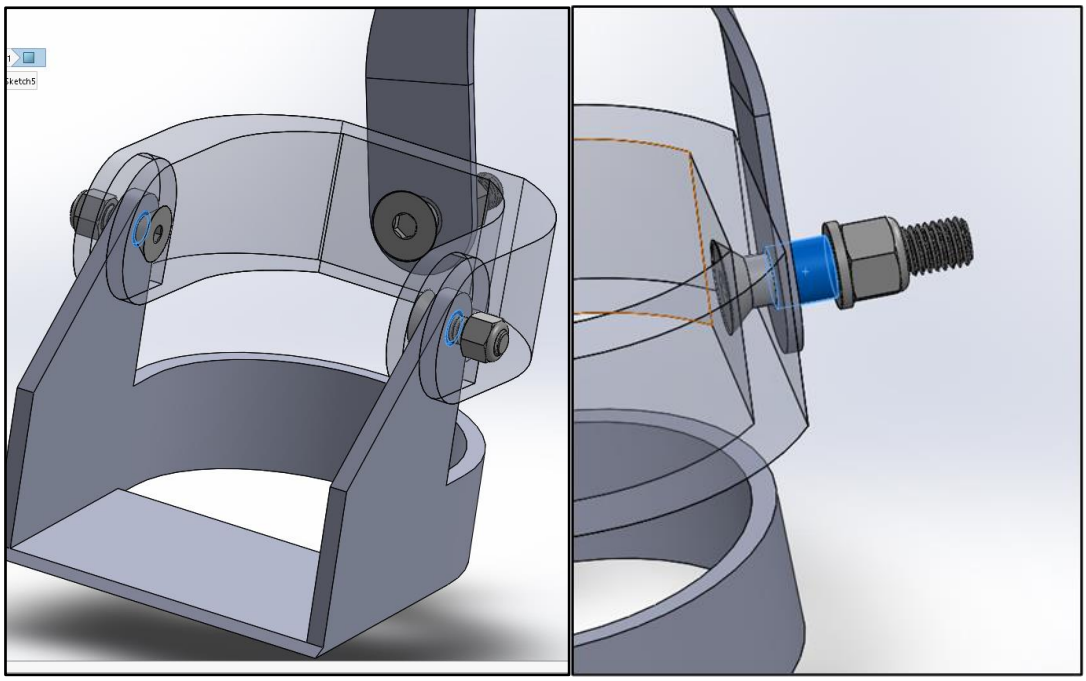

Figure 18: Ankle joint design developed in the fifth CAD iteration. Bearings are highlighted in blue.

CAD Iteration VI

The next iteration was centralized on the work on the band wrapping around the user's hip. It was decided that the developed exoskeleton would be attached to the user at the hips with a heavy duty climbing harness, therefore, there was a need for the hip piece to be moved higher up. This change would also create additional space where battery and wiring houses can be attached to the main frame of the exoskeleton (Figure 19). The desired outcome was achieved using two flat plates and vertical standoffs for the exoskeleton hip piece. The harness was meant to be attached via the holes in the center of the back, while a carabiner was intended to be attached to the last vertical standoffs on each side.

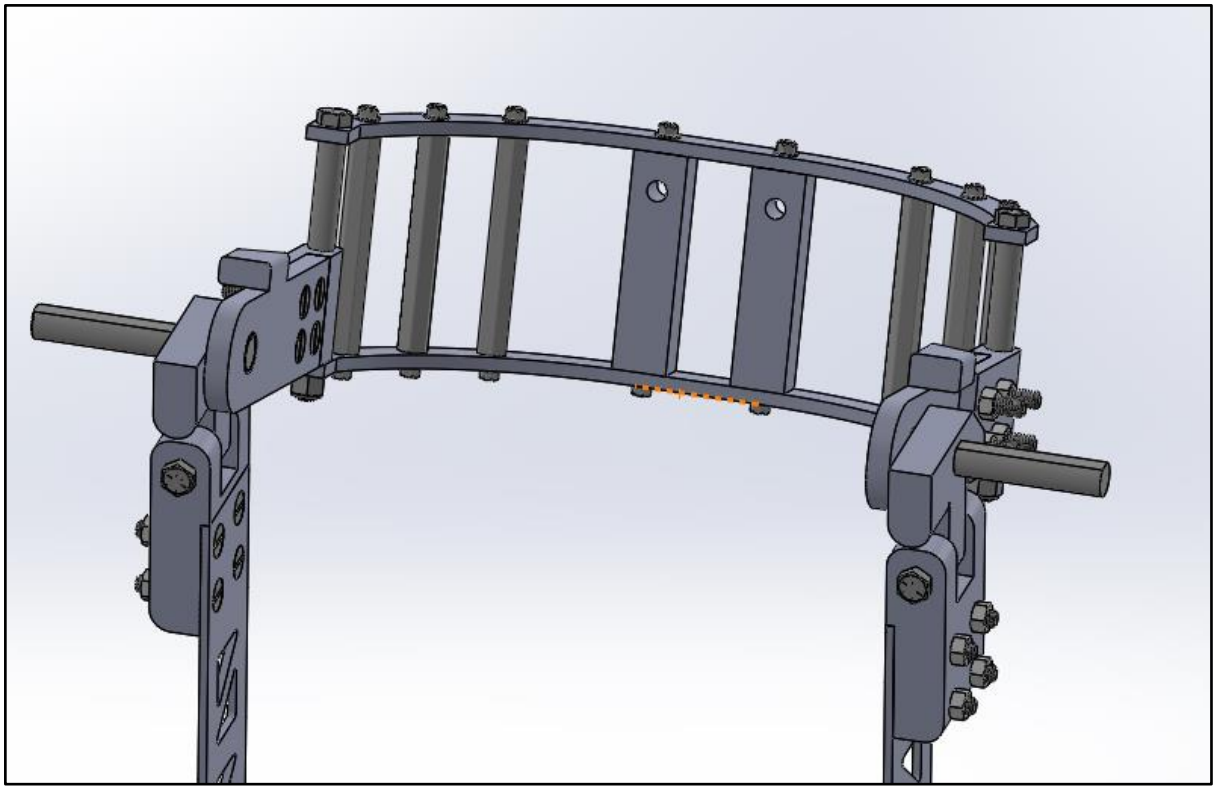

Figure 19: Back Support Design Developed in Fifth CAD iteration

Final CAD Design

Back Support

Since iteration six, the back support of the exoskeleton was redesigned to add rigidity to the part by creating a triangle on profile making it ergonomic on the inside while also acting as a better surface for mounting the hip gearbox and battery box. This geometry has increased load bearing capabilities. The triangular hole was also used for attachment of the harness to the exoskeleton.

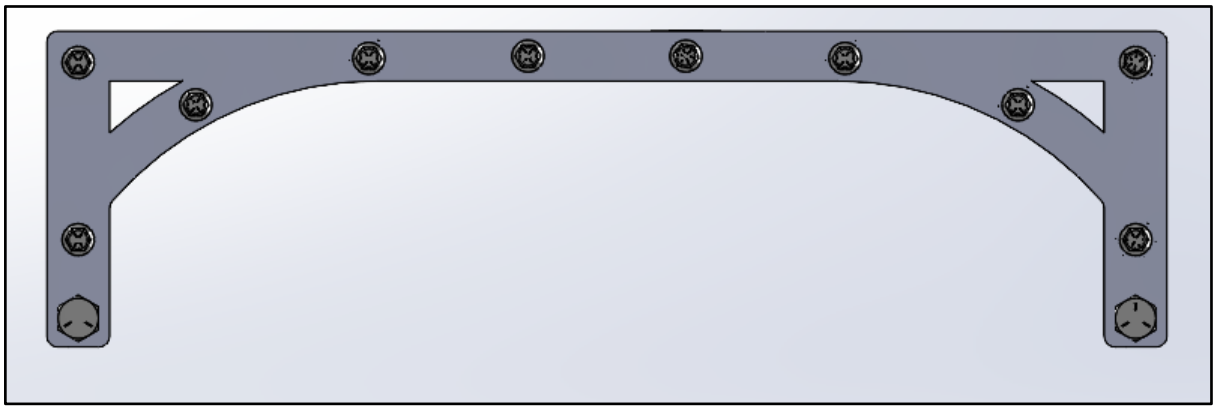

Figure 20. Final back support CAD design

Hip

The hip geometry was changed to add space for the mounting plate for the gear box. The hip part mounted to the back support was redesigned for manufacturability. The overhanging mechanical stop was removed and replaced with a plate that also acts as the gearbox mounting plate.

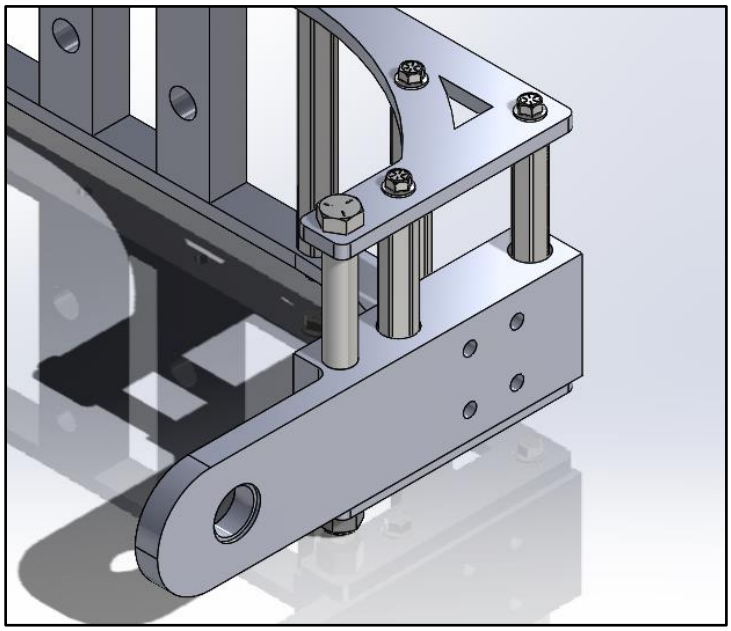

Figure 21: Final Hip CAD design

Hip Joint

In the initial cad, the hip joint was comprised of three parts. These three parts were redesigned with manufacturability and gearbox integration in mind. The final design reduced hip joint parts to two as the top of the femur part was removed. The T-shaped part of the joint was changed from a carbon fiber resin to sheet metal to interface with the gearbox better. A 316 stainless steel surface mounted hinge was added between top of femur and the hip to allow the leg to swing out. The femur and hip plates act as mechanical stop for the hinge when swinging in.

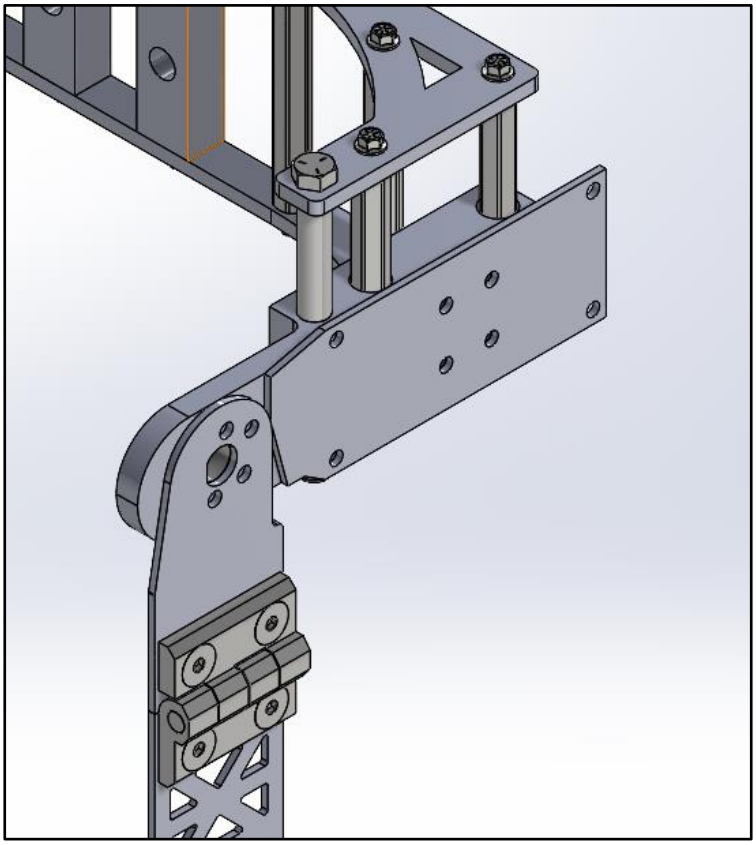

Figure 22: Final CAD Hip Joint

Femur

On the femur, attachment holes for the hinge and knee gearbox were added. The weight reduction cutouts were redesigned to maximize strength while reducing weight of the frame.

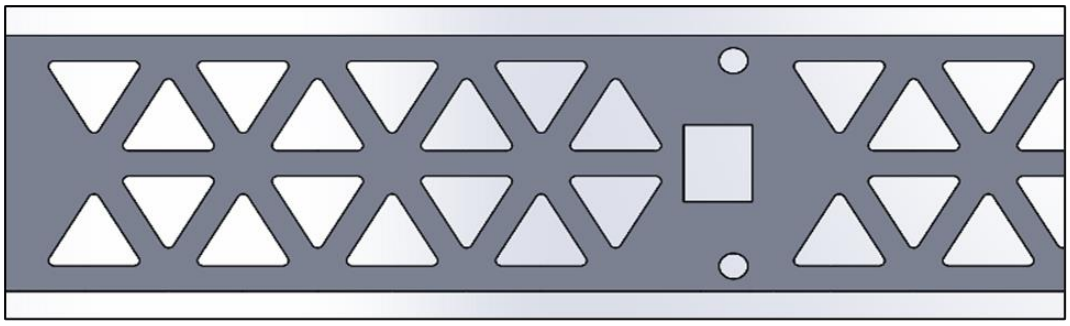

Figure 23: Femur Plate with Mass Reduction Cutouts

Knee Joint

For the knee, the weight of the mechanical stop and the inner knee plate was reduced by removing unnecessary geometry towards the top of them serving no purpose. A thrust bearing was

added into the inner knee plate for friction reduction between the shaft and the plate. We also made the flexion hard stop angle 110 degrees instead of the previous 90 degrees.

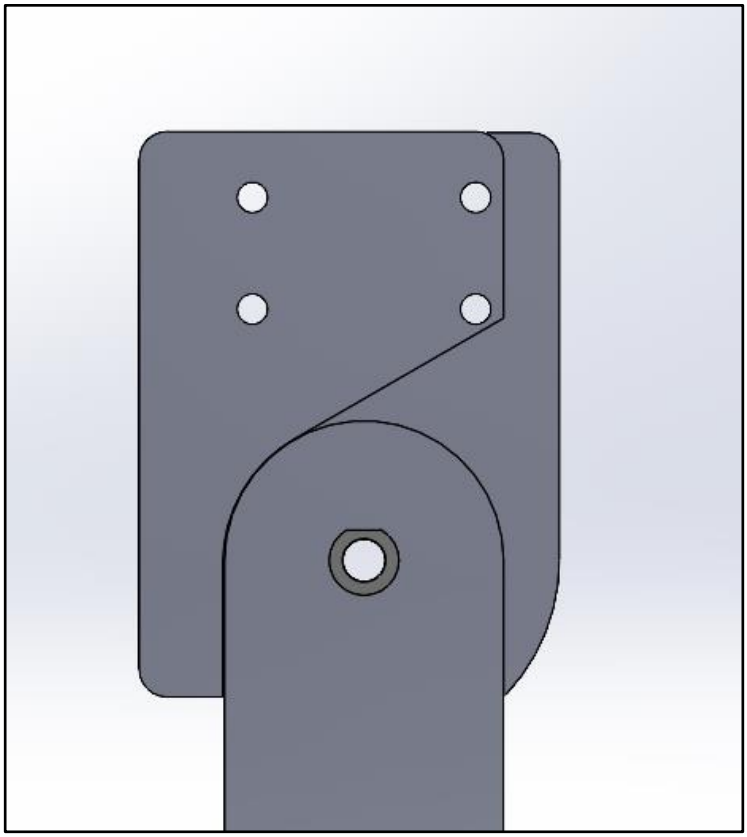

Figure 24: Mechanical stop at the knee joint

Calf Spline

The thickness of the calf spline was increased and the cross sectional area was made uniform throughout the twist to reduce stress concentrations. This part was designed with the manufacturing process of a carbon fiber resin mold in mind.

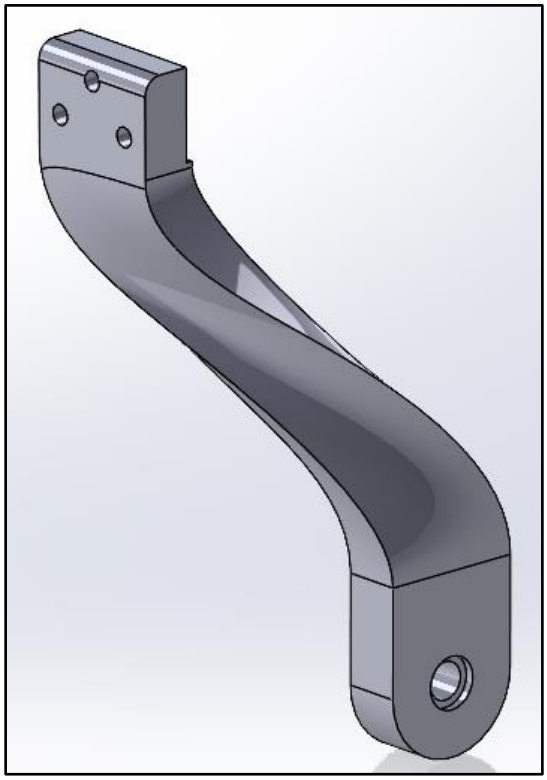

Figure 25: Calf spline

Heel cup

The geometry of the heel cup was changed to increase manufacturability (ability to release from mold). A small plate on the outside of each side of the heel cup was added also. For positioning purposes, potentiometer mounts were added to the ankle joint of the heel cup.

Foot Base

The foot base was redesigned into four parts for manufacturability: two water jet cut, one carbon fiber resin molded, one 3D printed from Polyethylene terephthalate glycol (PETG). The side plates on the outside of the heel cup were waterjet cut out of steel plate. The part of the base that wraps around of the back of the soldier's boot is carbon fiber resin. The cross bracing triangular geometry was 3D printed using fused deposition modeling (FDM) with PETG.

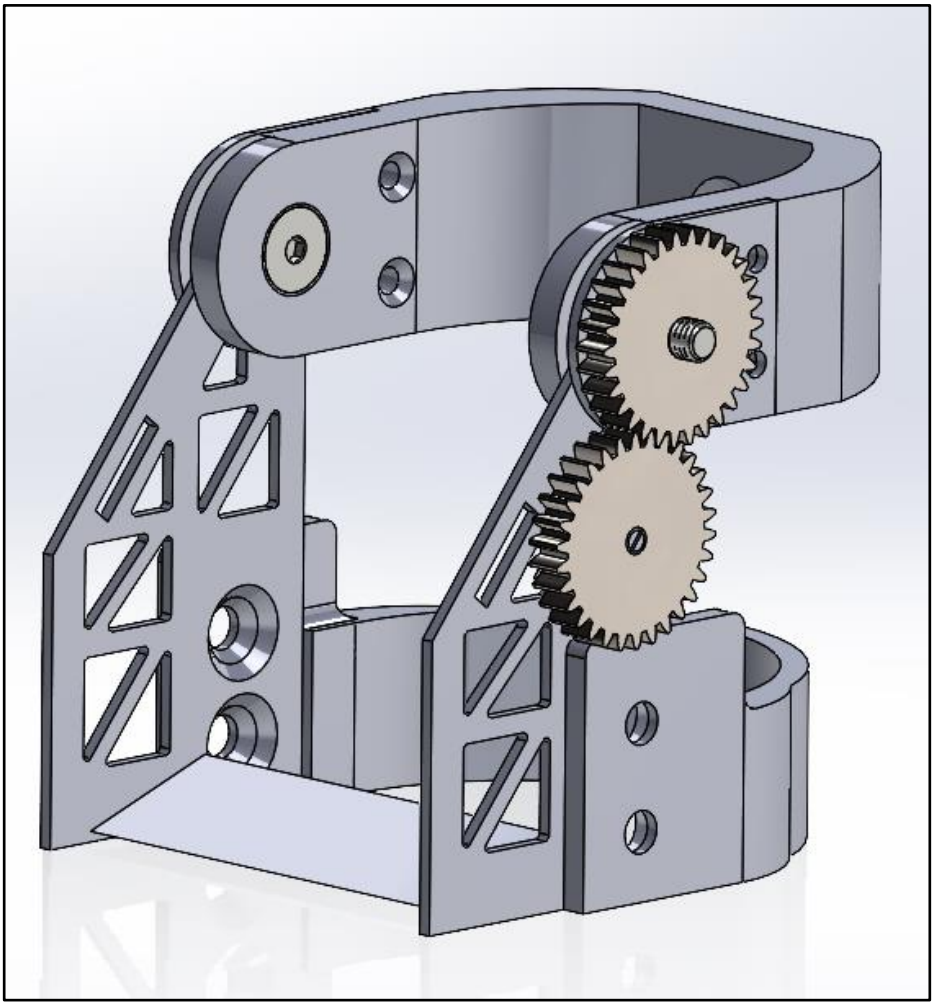

Figure 26: Final heel cup and foot base CAD design

Knee and Hip Gearboxes

A singular gearbox is comprised of 44 individual components. The gearbox contains a three-stage gear ratio increase of 1:25.4. It is manually clutch engaged/disengaged and spring assisted. When the clutch is disengaged, wave springs separate the clutches allowing for operator use without the need to backdrive motors in the event of a dead battery or controls/ electrical issue.

The knee and hip gearboxes are nearly identical except for the spring insert, which is slightly different in how it interfaces with the frame to transfer torque from the torsion spring force. The spring exerts 2.43 in-lbs per degree of rotation with a maximum rotation of 240 degrees. The spring transfers its torque with the yellow spring engager in Figure 27. This part is made of PLA but has holes within it that ¼ inch steel rods fit through and holes in the gearbox and frame to successfully transfer torque. The shaft can spin freely within the spring engager to either be driven or act as a passive shaft. The casing is made of PLA and primarily acts as a standoff for the through bolts and

protects the user from clothing or fingers getting caught in the gears. The casing has a slot in it that allows the user access to the clutch engager.

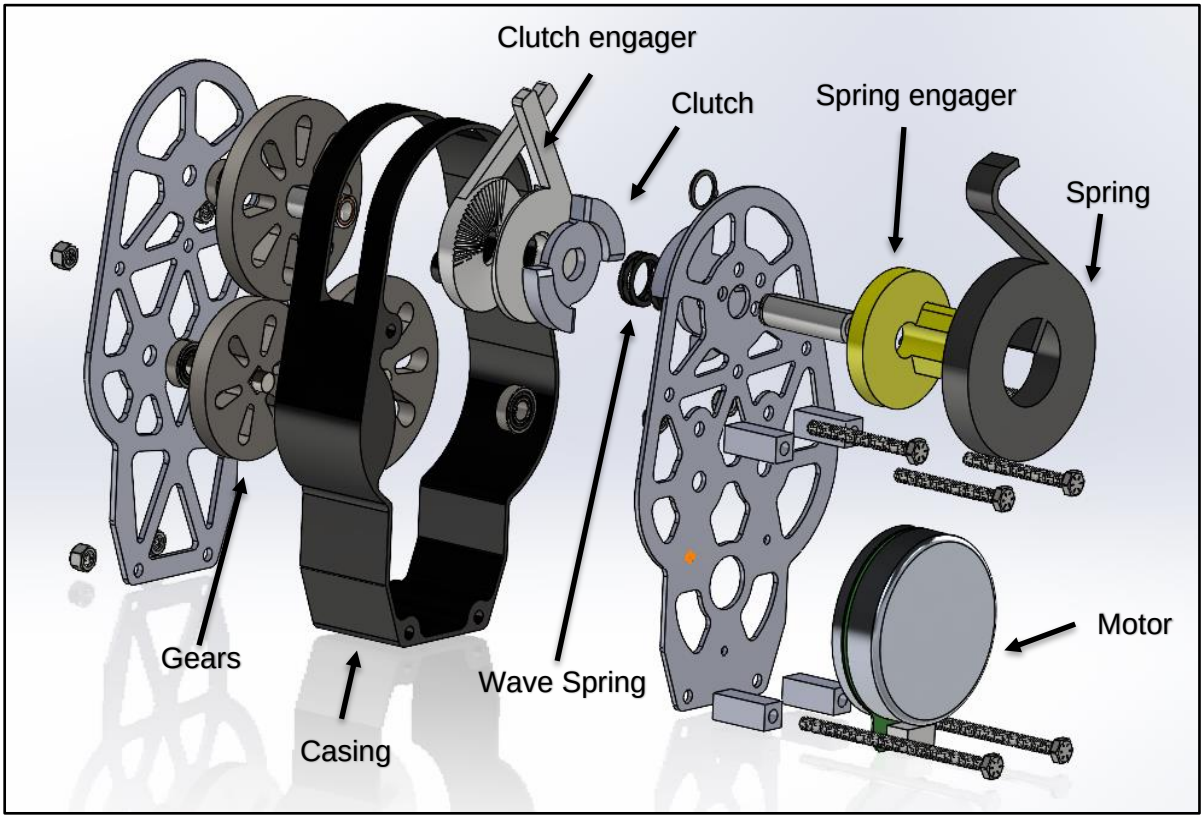

Figure 27: Final Gearbox CAD exploded view.

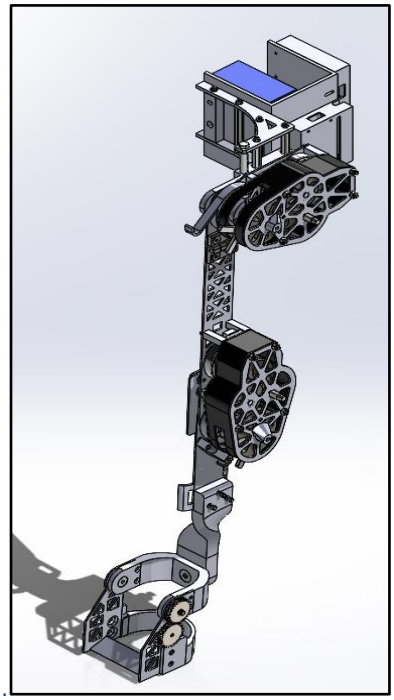

Figure 28: Section View of the full assembly

ANSYS Simulation

ANSYS® is a finite-element modeling software that can be used to model the strain and stresses on a part based on the forces applied to it. As part of the verification of the developed CAD model, this software was used to perform the static structural analysis of the components of the exoskeleton frame. Each developed joint was simplified in the originally used CAD software to remove extraneous features that were complicated but did not add to structural integrity. This procedure was performed for all necessary structural components of each section of the exoskeleton. Figure 28 demonstrates an example of the simplified CAD model of the hip joint imported into the ANSYS® software.

The ANSYS® simulation set up included suppressing all fasteners as this is greatly simplifies the computation model that needs to be solved. The fasteners add too much complex geometry for an area that is not of focus in these simulations. All five contacts were set as bonded contacts. This is another simplification for the finite element analysis. A fixed support connection was assigned to the bottom five knee attachment holes. A cylindrical support was added to the interior faces of "door hinge" joint at the hip. A force of 535 Newtons applied on the top face of hip part (eccentrically loaded column). The 535 newtons was determined by finding the bodyweight force of half of one soldier (~90 lbs) since this simulation is for only one side of the exoskeleton. Figure 28 demonstrates simulation set up.

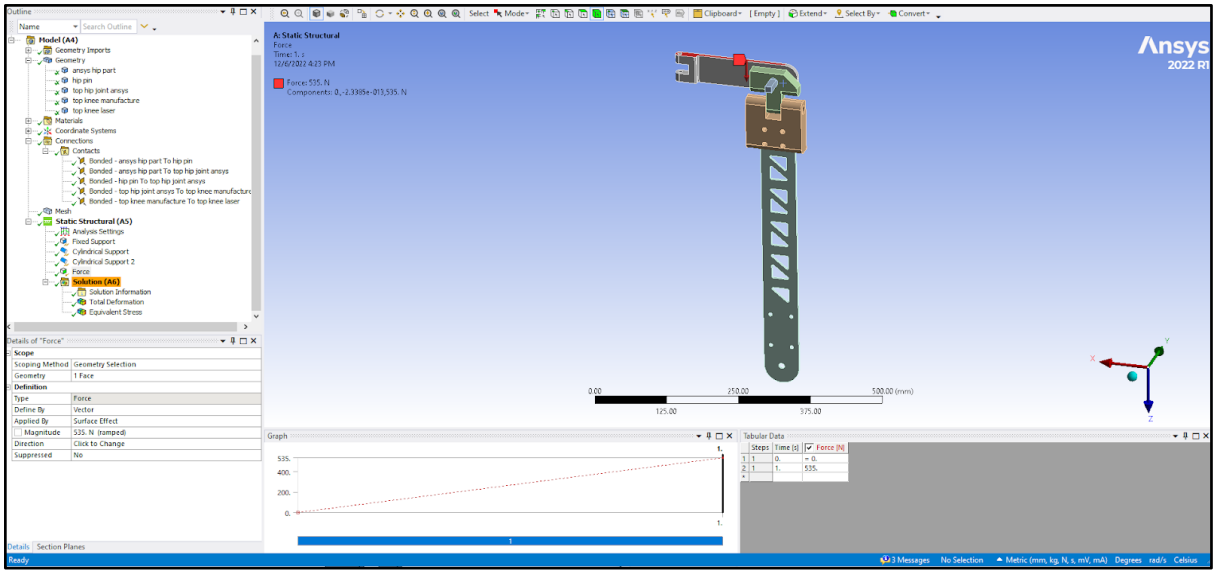

Figure 29: Set up of ANSYS® simulation on hip joint

Results of the ANYSYS® total deformation simulation can be seen below in Figures 29 and 30.

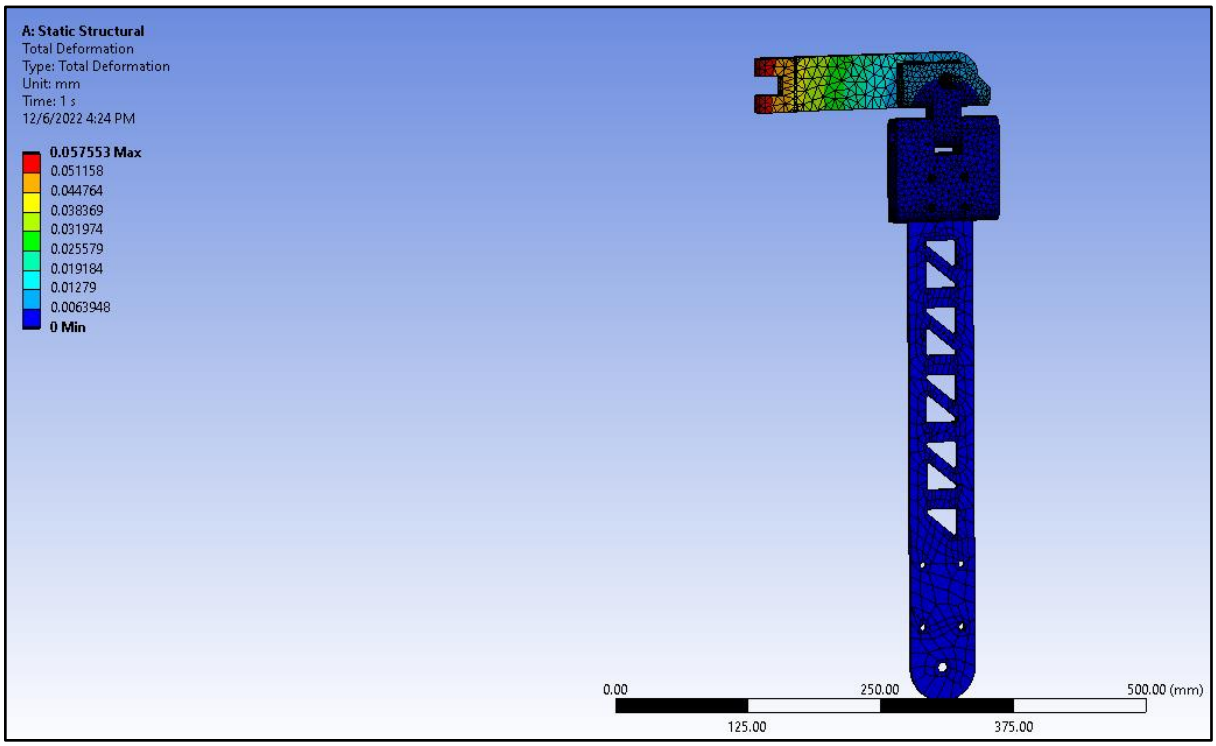

Figure 30: Results of the ANSYS® total deformation simulation for the simplified CAD of the hip piece. The red region is the area of largest deformation in mm.

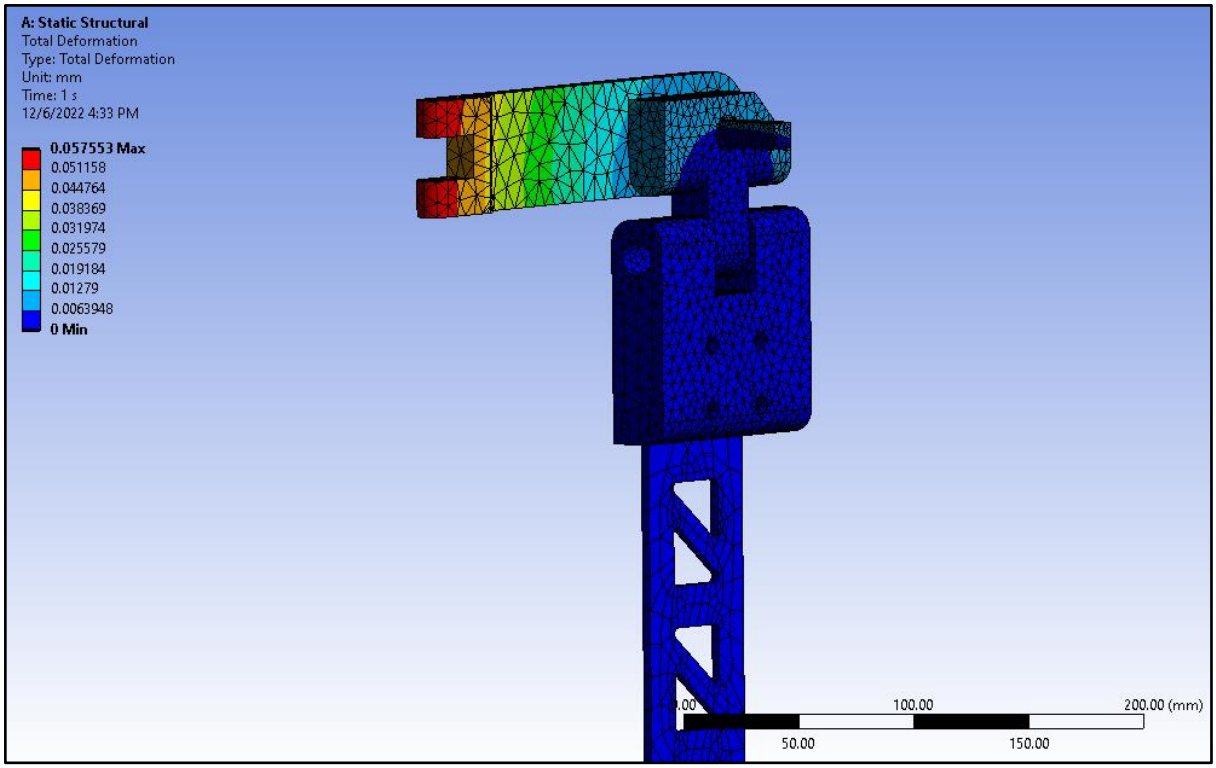

Figure 31: Enlarged results of the ANSYS® total deformation simulation for the simplified CAD of the hip piece.

The maximum theoretical deformation of the hip piece was approximated to be 0.058 mm. Under these boundary conditions, the top of the hip part acts as a cantilever beam that makes the largest deflection occurr at the end of the hip component that doesn't have a fixed support. Therefore, this deflection value was considered negligible.

The simulation was also run to find the Von Mises Equivalent Stress. The equivalent stress is a measure of the combined effect of normal and shear stress in a material. It is used to assess the structural integrity and failure criteria of components subjected to complex loading conditions. Results of the ANSYS® Von Mises Equivalent Stress simulation can be seen below in Figures 31 and 32.

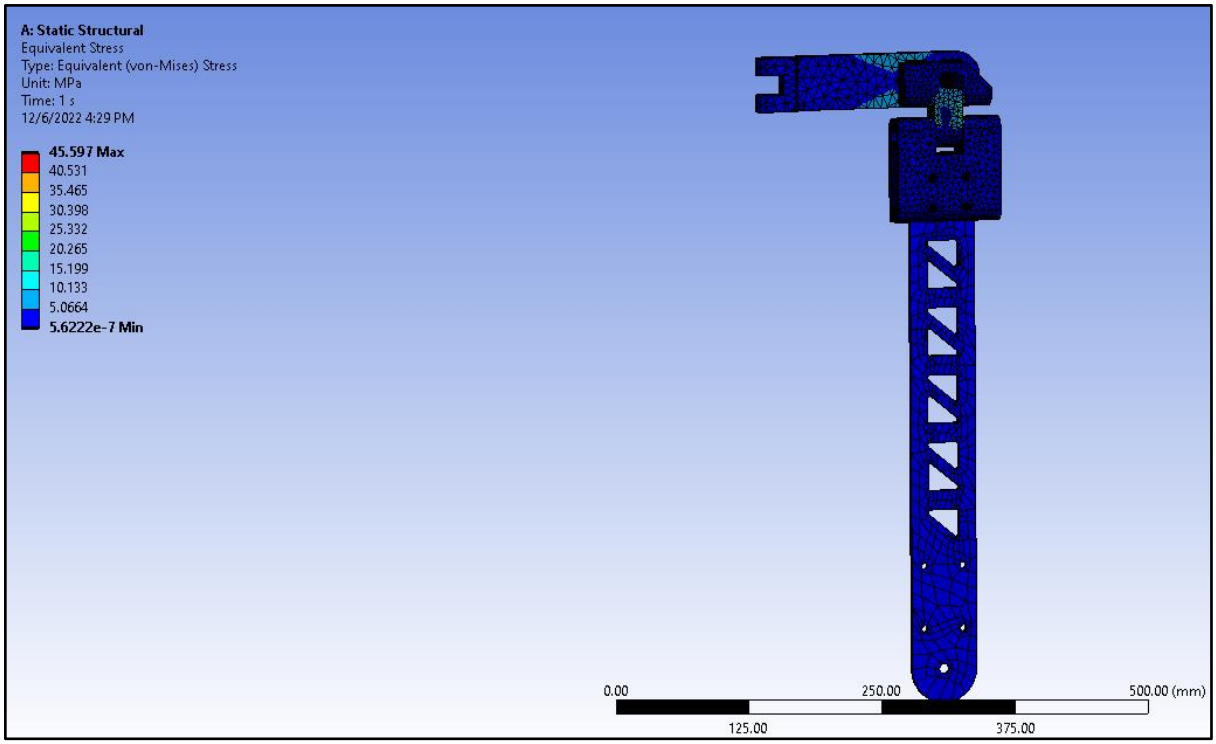

Figure 32: Results of the ANSYS® Von Mises Equivalent Stress simulation for the simplified CAD of the hip piece. The red region is the area of largest stress in MPa.

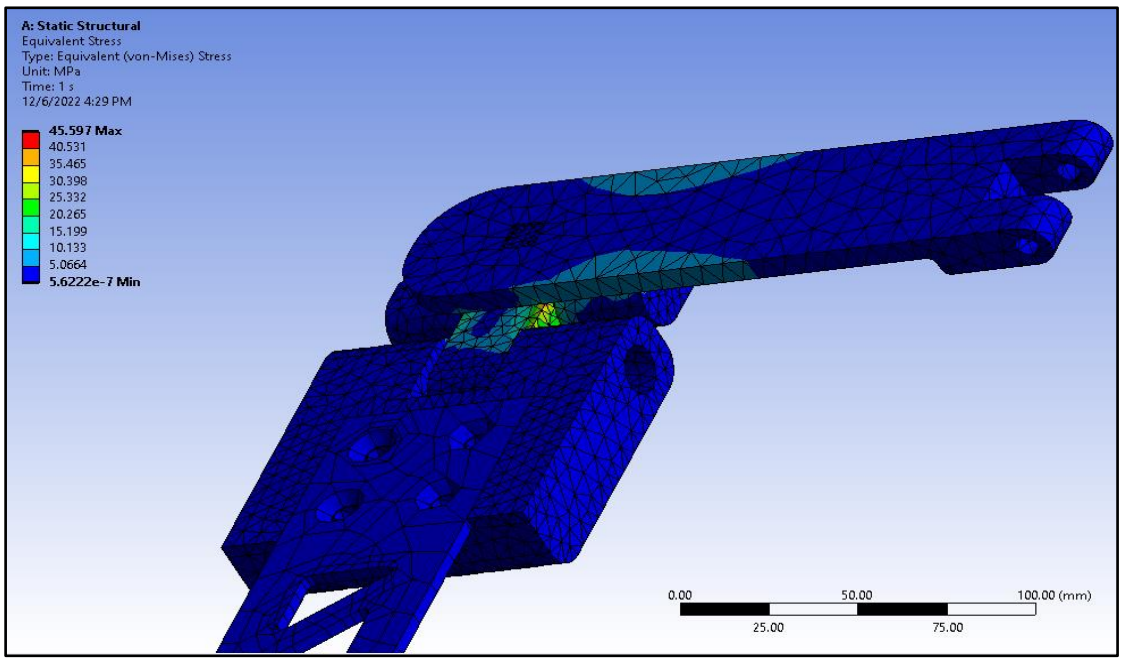

Figure 33: Enlarged results of the ANSYS® Von Mises Equivalent Stress simulation for the simplified CAD of the hip piece.

The maximum equivalent stress was found to be 45.597 MPa. This maximum was identified on the edge of a sharp corner in the geometry that was produced as a simplification in the connection

contact of the “door hinge” joint. This value of 45.6 MPa is significantly less than the yield strength of 250 MPa for mild steels, therefore, this number was considered negligible. After ANSYS® analysis was completed, the developed exoskeleton design was acknowledged as verified and manufacturing stage was begun.

Manufacturing

Water Jet Cutting

Once the final design was complete, the manufacturing phase of the project began. To start, ideas were brainstormed on how to most efficiently manufacture each piece. It was decided that the plates could be rapidly produced if they were to be taken to a Hydrocutter. This also allowed for a more complex design within the plates to reduce weight. These plates were made from A36 steel, a strong and durable metal.

Figure 34: Hydro cut plates

Milling

For all the milling and turning operations, Autodesk Fusion 360® was used to produce NC code for each piece. This allowed for a smooth transfer of a SolidWorks® file into Autodesk Fusion 360®, which then gave the Mills and Lathes the correct information to produce each piece.

Since the waterjet had a cutting tolerance of +/- 0.002 inches, it was decided that where bearings needed to be press fit, they would be post-processed. This would entail milling them out to the exact dimension. In order to do this, fixture holes were incorporated into the plate design and these holes were used to mount each plate onto a fixture plate that was designed and manufactured. With this fixture mount, all 8 plates were able to be quickly manufactured so that the bearings could be press fit when inset into the plates.

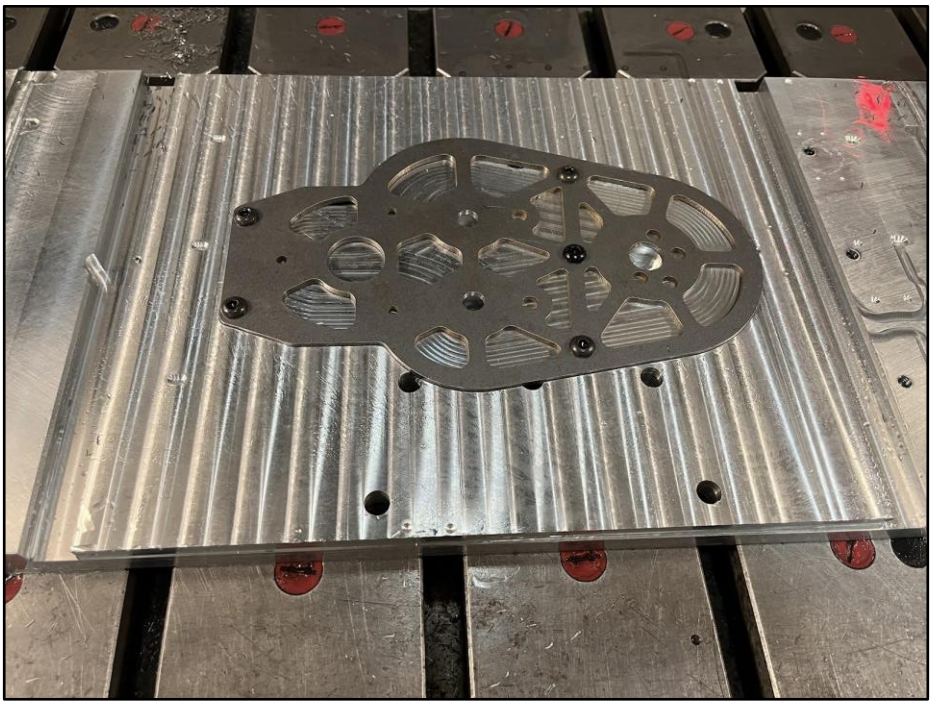

Figure 35: Knee Gearbox plate on our Fixture mount

Another piece that needed to be manufactured was the two hip pieces that connect the gearbox to the back support. These two pieces were produced in 3 operations on the mill, using 6061 aluminum stock. This allowed for a lightweight piece that was still able to support heavy loads.

Figure 36: Hip Pieces mounted to back support

In the big push to reduce weight, it was decided that milling down the gears from last year's MQP could be an easy way to achieve this. In this process, soft jaws were created that would allow for the gears to be placed within the jaws directly, and then each side of the gear could be milled. This reduced the weight of each gear by 40%, reducing the overall weight of the exoskeleton by 10 pounds. Below is a picture of the new gears compared to the old gears.

Figure 37: New gear on the left with old gear on the right

Turning

Another part that needed mass manufacturing were the eight D-shaft pins used in the gearbox to activate the clutches. Due to the D-shaft, these parts were difficult because they were tough to probe correctly. In order to fix this, they ended up being produced in the lathe. The shafts were first cut to the exact length with +/- 0.001 inches. Then with a hard stop in the fixture, the operation was run four times and quickly produced each shaft. Six out of the eight shafts needed two operations, due to their features close to each end. Below are the three different kinds of shafts produced. The 4 shafts with square ends were made in the Mill-turn.

Figure 38: Clutch engaging shafts

One of the more complicated pieces to manufacture were the clutches. With the need to be perfectly centered while also maintaining a D shaft in the center, it was a challenge. In order to efficiently complete this operation we ended up making it on the millturn, a machine that incorporates both the aspects of the lathe and the mill. Adjustments had to be made to allow for the D to be

inscribed into it, but it still served its purpose by not letting the D shaft rotate within it. Below are two pictures of the clutches, showing them alone and also how they operate together on a shaft.

Figure 39: Individual clutches and assembled together on a shaft.

Carbon-Fiber-Reinforced Resin

After some consideration, it was concluded that the design of certain exoskeleton parts was too complex to manufacture with any methodology indicated above. In order to resolve the emerging issue, it was decided to try a novel method of carbon fiber reinforcement (CFR) manufacturing. With respect to its low density, CFR resin demonstrates incredible yield and tensile strength, as well as durability and water-resistant properties, making it ideal for wearable devices such as the exoskeleton (S. Sádaba, 2015).

Manufacturing from CFR resin involves 4 main steps that are mold production, mold filling (resin application and addition of carbon fiber), curing, and post-processing.

1. Mold production

   The first step in the manufacturing process of reinforced carbon fiber parts was to prepare the mold. The mold was created using computer-aided design (CAD) software, Solidworks®, which was used to design the shape and size of the exoskeleton part. Once the design was complete, the mold was then 3D printed using either a high- or low- resolution 3D printer, depending on the size and complexity of the desired shape. After, the mold was cleaned and

polished with acetone to ensure a smooth contact surface. The polished mold was lubricated with petroleum jelly to facilitate the process of the release of the cured piece.

2. Mold filling
    a. The next step was to apply the resin to the mold. In this case, a two-component thin epoxy from US Composites was used (635 Thin Epoxy System, US Composites, USA). Resin and medium epoxy hardened were mixed together in a 3 to 1 ratio and then applied to the mold using a brush. The resin was applied in a thin, even layer to ensure proper adhesion of the carbon fiber to the mold.
    b. Once the resin was applied, the carbon fiber chops were added on top of it (½" Chopped Carbon Fiber, Venom Carbon, USA). The carbon fiber chops were placed over the resin layer and pressed down with a wooden stick to ensure its adhesion. Described steps were executed repetitively until the desired thickness was achieved.
3. Curing

    The next step was to cure the carbon fiber and resin. In the case of the technology used in this case, the curing was happening under elevated pressure. The desired pressure was achieved by the placement of the closed mold in strong mechanical clamps. The temperature and time required for curing depend on the type of resin and the thickness of the carbon fiber, however it never exceeded 16 hours.
4. Post-processing

    Once the curing process was complete, the carbon fiber and resin mixture was hardened, resulting in a strong and durable exoskeleton part. The final step was to release the part from the mold, trim it from any excess material, polish it to achieve a smooth finish, and cover it with a thin epoxy layer for additional durability.

Figure 40: Completed carbon fiber resin calf spline.

Assembly

The final step was the assembly of the exoskeleton and attachment of the electrical components such as the battery, force sensors, and motors. It was assured that all mechanical parts were properly aligned and secured, while the electrical components were properly integrated into the exoskeleton's design.

Within the assembly phase, there were some minor unexpected issues that needed to be addressed. The first issue was the fit of the D-shaft housing within the hip plate. Due to the tolerancing of the hydrocutter, the D-shaft sat loosely as a clearance fit. This caused the D-shaft to be able to gain momentum while rotating within the hip, causing it to shear through the hip plate. In order to fix this, new plates were hydrocut with a tighter tolerance, ensuring a transition fit. This allowed for the D-shaft to sit perfectly within its housing, and with no fear of unwanted movement. As a second layer of protection, the D-shafts were also welded to the hip plates. Due to the tight vertical tolerancing between the hip plate and the gearbox, the weld could have a maximum thickness of 1/16 of an inch. In order to achieve this, each weld was hand filed in order to preserve the shaft while reaching the desired goal. This welding process was also applied to the knee plates as a safety measure.

A second drawback that was found in the assembly phase was on the steel plate of the femur and the tibia. Throughout the pressure applied to them in the assembly phase, they both started to

slightly bow out. To fix this issue, aluminum angle steel was added on both sides of the longer femur and on one side of the tibia.

Figure 41: Tibia angle aluminum

With the addition of these angles, the leg strap holder was no longer able to be attached on the plates. To fix this issue, holes were added into the angle aluminum where the velcro straps could be fed through.

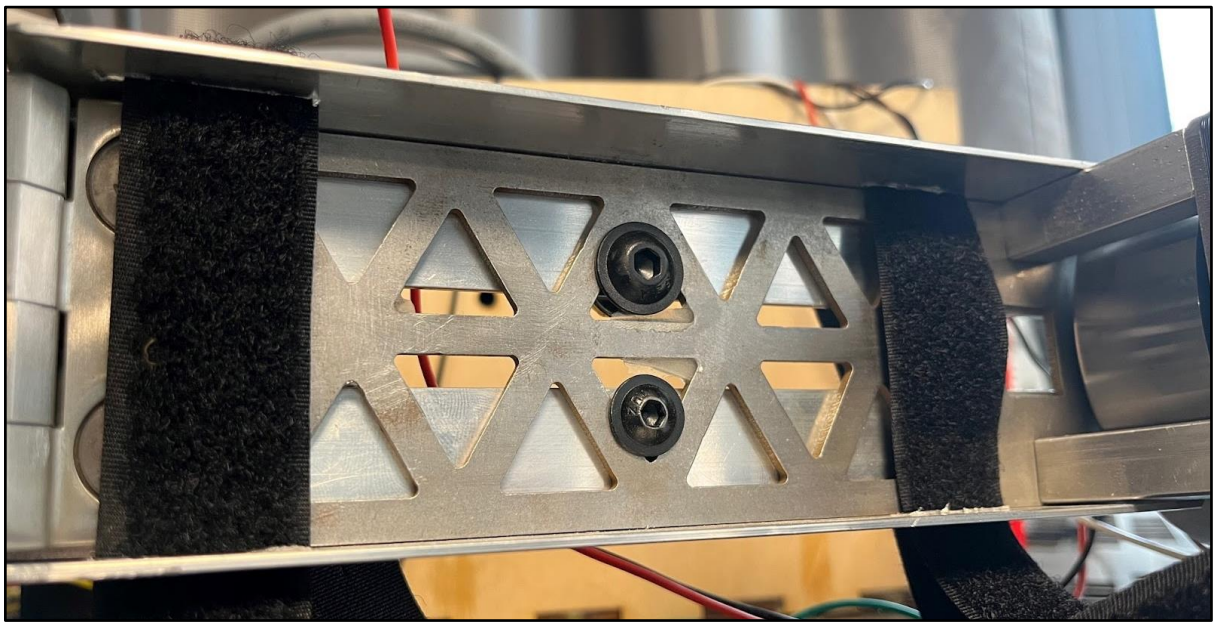

Figure 42: Femur Aluminum Angle with Velcro Strap Holes

A third issue that was encountered was the friction between the D-shafts in the clutch engaging mechanism. The way that the system was designed, the bottom D-shaft has a smaller ⅜ inch diameter pin that would sit concentrically within a slightly larger hole in the top D-shaft as shown above in Figure 37. This would allow the two to sit together while still being able to rotate independently. Due to the aluminum sitting within aluminum, the friction was causing the D-shaft to get stuck and would stop the independent rotation. To fix this issue, a larger hole was milled into the top D-shaft and a ½ inch oil embedded bushing with a ⅜ inch hole was press fit into it. This allowed the bottom D-shaft to freely rotate with very minimal friction.

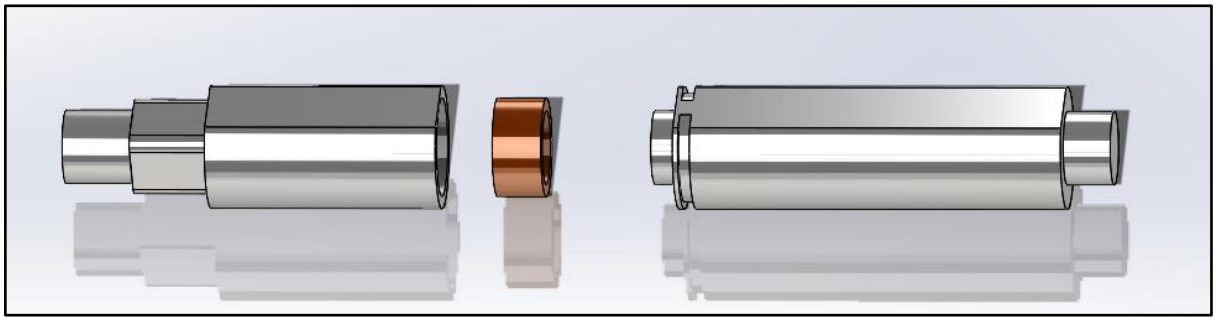

Figure 43: D-shaft with Bushing Housing and Bushing

Circuit Design and Electrical Component Selection

The circuit for the exoskeleton project was designed using Altium Designer®, which allowed us to create a clear and organized layout of the components and all I/O connections. The design was based around our requirements for controlling the motors we were given from last year's project, and we carefully selected a range of electrical components to properly support them.

The main components of the circuit included an emergency stop button, potentiometers for motor positioning, motors, motor controllers, a microcontroller, and a battery to power the motors. The specific microcontroller used was an Arduino Mega that reused from the previous project and it was perfectly capable of handling all of the sensors and processing needed. It was powered by a rechargeable 9V battery, which provided a convenient and reliable source of power for the microcontroller and other components.

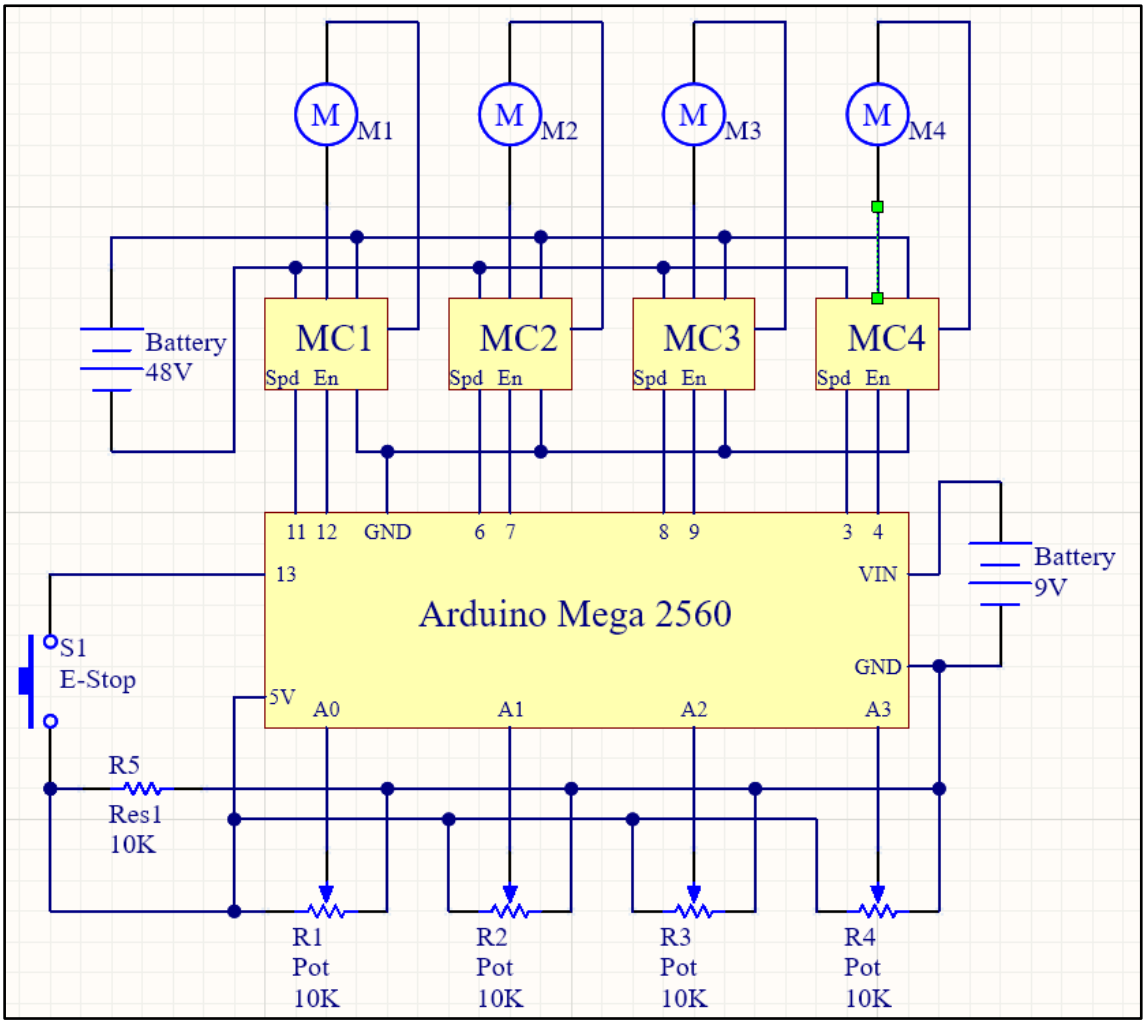

Figure 44: Final Circuit Design

The emergency stop button was a critical safety feature in our exoskeleton design. It was constantly being digitally read by the Arduino and connected to the circuit through a 10k ohm pull-down resistor. When pressed, it immediately set all motor enables to low to stop them, and was used both for testing and for the wearer to hold. We made sure to include a pull-down resistor to ensure that the circuit remained in a safe state in the event of a disconnection or failure of the button.

The potentiometers were used to control the positioning of the motors and were analog read by the microcontroller, with a range of 0 - 1023. We had a motor controller for each motor, the motor enables were set with a digital output and the motor speed was set with an analog output in the range of 0 - 5V. This allowed us to fine-tune the movement of the exoskeleton's legs and achieve precise speeds. The motor controllers were given to us by the same company that makes the motors so using them together worked really well.

Our battery was a critical component of our circuit, as it provided the power to drive the motors. It was a 20Ah, 48V lithium battery designed for electric bikes, which provided a high energy density and long runtime. We chose this battery due to its high capacity, the correct amount of voltage for the motors, and relatively low cost compared with other options that met our needs.

To ensure that each component was working properly, we tested them individually with a digital multimeter before integrating them in the final circuit. This included testing the E-stop by triggering an LED to confirm its reliability. The voltage of the battery was tested both on a full charge and as it depleted to ensure it was within the required operating range. We also ran all four motors with the battery to confirm it had enough continuous output current to power all of them together. The resistance of each potentiometer was measured to know that they were all linear and that they had the same resistance range.

Overall, our circuit design and component selection were critical to the success of our exoskeleton project, ensuring that it could operate safely and reliably. We made sure to take into account the power requirements, safety features, and control systems needed to achieve the desired motion of the exoskeleton's legs. Through careful selection and testing of the electrical components, we were able to create a robust and effective circuit that met our project goals.

Code Implementation

The code running on the Arduino for the exoskeleton involved position control to ensure smooth and accurate movement throughout the gait cycle. This positioning was done using proportional derivative control. We were able to get acceptable results in the positioning testing using just the P and D terms without having to include I for the integral term. Independent PD values were used for each motor in both forward and backward movements to account for variances. These included needing more torque at the hips given the weight of the full leg, gravity and the springs helping to straighten the leg, and differing tightness and dead space in each gear box.

$$m(t) = K_p\, e(t) + K_D \frac{d}{dt} e(t)$$

Figure 45: PD control output formula

To accurately determine the angles of each motor, on initialization the code zeroed each potentiometer and converted the readings to angles. This was necessary given that all potentiometers were in differing positions on startup. The potentiometers had 300 degrees of rotation, so the readings were converted to angles with this equation: 300/1024 - initial reading. The goal angles for hips and knees both forward and backward were determined from a motion study and tested with 25 degrees forward and 5 degrees backward for the hips, and 0 degrees forward and 20 degrees backward for the knees.

To ensure smooth gait movement, the code triggered a leg direction switch in the cycle when all four motors were at their designated angles within a given threshold. Throughout testing we found that a threshold of 3 degrees was a good value to ensure consistency without hindering the direction switching. Once all motors reached their designated angles, they would switch to the designated goal angles in the other direction.

The control loop had three main parts. The first was checking the E-stop status, keeping track of the reading, and setting all enables to low if the button was pressed. The second was performing the calculations that were used to determine the current motor angle and the errors in the current angle to

the desired angle. This also involved assigning the according PD constants, and calculating the desired PD value for the motors. The code then checked if all motors were at their designated angles to trigger direction switching. The third part was actually moving the motors. The motors were moved depending on their currently assigned direction. With the desired angle set and the calculated PD output, it was remapped to 0-255 range and then analog wrote to the motor controller. To ensure safety, maximum angles were set in the software, and all motors would be disabled if the current angle was somehow outside of the max angle range.

To test the code, the e-stop check function was verified by testing with a single motor. PD control for positioning was also tested on a single motor before mounting it onto the exoskeleton. Checking motor angles was done by manually moving the leg while reading out the current angle measurements and comparing them against markings on the exoskeleton. The final test involved a full cycle on the actual exoskeleton running all four motors through the gait cycle while the exoskeleton was mounted to a table.

Exoskeleton Control System

Potentiometers for Position Sensing

In order to sense the positioning of the exoskeleton it was outfitted with four Dafurui ® B10kOHm rotary potentiometers. Originally, the positioning was going to be handled with the use of hall sensors that are built into the Maxon ® 500267 and 500269 motors, but through rigorous testing, it was determined that the built in hall sensors were not accurate enough for the application at hand. The rapid movement back and forth of the motor combined with the high torque associated with the varying loads of the legs skewed the readings of the hall sensors to a point where they were unusable, causing us to pivot to the potentiometer approach.

These potentiometers were chosen for their ability to rotate 300 degrees and linearly report their data. Linear potentiometers are essential for this application due to the precise nature of the angle readings that are reported from the end of the shaft. The length of these potentiometers was 3.1 centimeters which allowed the potentiometer to be mounted into a custom modeled 3D printed

potentiometer mount which was press fitted directly to the end shaft on the gearbox with the potentiometer in it. The potentiometer was directly connected to a common 5 volt supply from the Arduino ®, and was read via analog pins in the Arduino ® board.

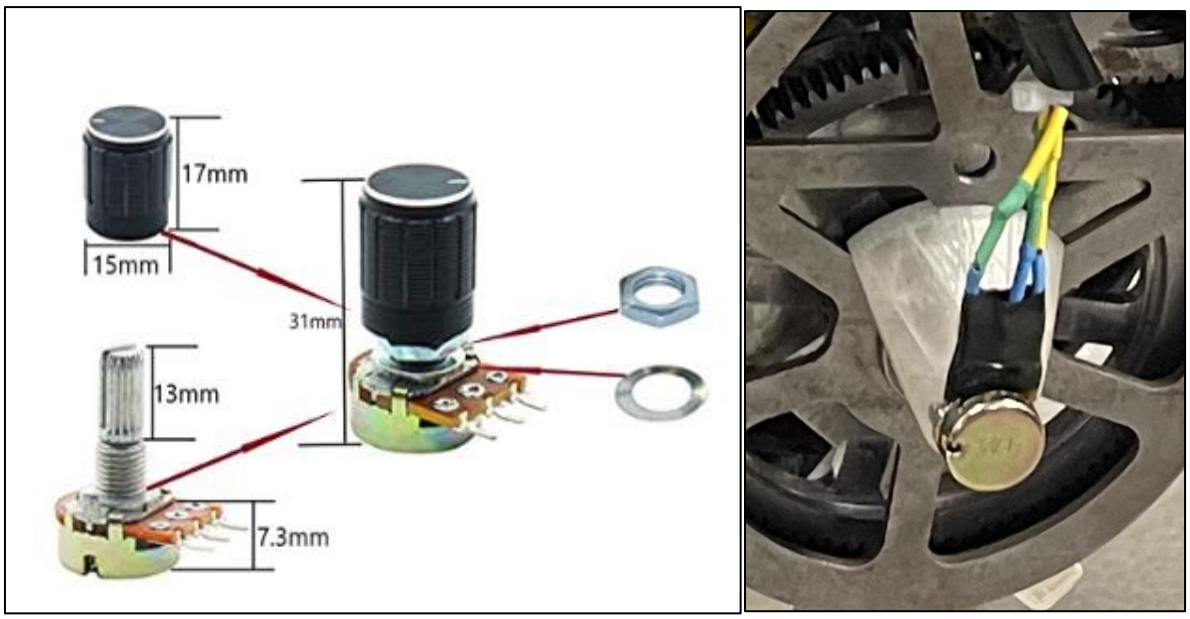

Figure 46: Dafurui B10kOhm Potentiometer, and Mount to Gearbox Endshaft

Motors

The motors used on the exoskeleton were two Maxon® EC90 Flat 500269 motors, and two Maxon® EC90 Flat 500267 motors. The two 500267 motors were from last year's MQP, and so it was decided to continue on using these motors due to their complex range of useability and built in hall sensors.

The 500267 has a nominal voltage of 48 Volts, and a nominal current of 4.06 Amps with a stall torque of 13100 mNm. The 500269 has a nominal voltage of 18 Volts, and draws a nominal current of 12.1 Amps with a stall torque of 14800 mNm (Maxon®, 2021). It was concluded through the motion study that the knee would require more torque in order to operate the system fluidly, and so it was determined that the Maxon® 500269 motors should be placed on the knee.The 500267 motors would then in turn be placed on the hip, which requires much less torque to operate.

These motors come equipped with Maxon's® on board hall sensors that the motor uses in three stages in order to calculate position, speed, and direction of rotation. Through the use of code based inputs from the Arduino, the motors can be controlled in all of these aspects, while outputting the values of these aspects to the Arduino for further evaluation in the code.

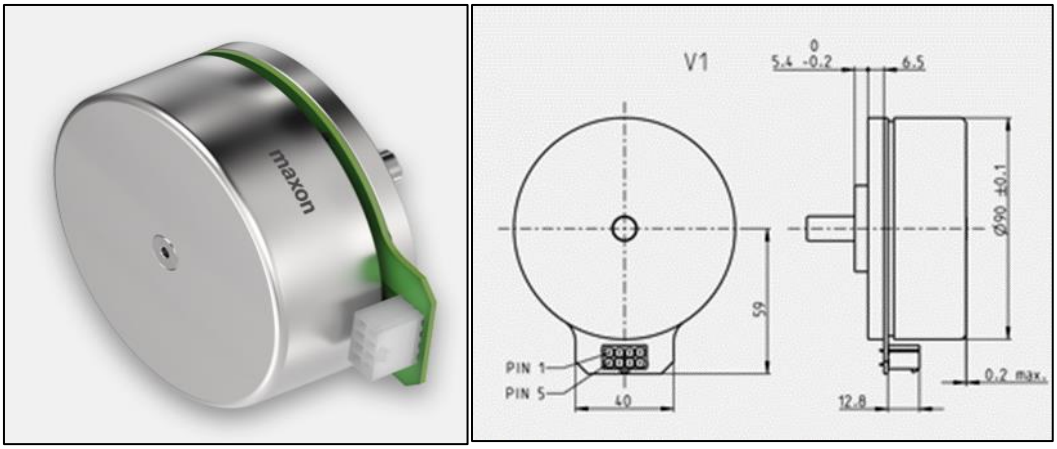

Figure 47: The Maxon EC90 Flat 260W Motor

Motor Controllers

The motors are directly controlled by two sets of two motor controllers from Maxon®. The Maxon® 409510 can operate in a range of 5 to 50 Volts with a current draw of 5 to 15 Amps maximum, making it ideal for the application of the 500267 motor, which needs a supply of 48 Volts to work properly, and draws a current of around 5 Amps while operating. In turn, the knee motors which require less voltage, but much higher current are controlled with the 422969 70 volt range motor controller, which can withstand a current draw of up to 30 Amps (Maxon®, 2021).

The motor controllers themselves are a versatile tool that can be used in a broad range of applications with the motor. The motor controller contains 6 analog I/O ports, 4 digital I/O ports, a hall sensor connection, motor winding pin connectors, and the overall power supply connector. The analog I/O pins are versatile in allowing the controller to output many readings from the hall sensors which include but are not limited to: current speed, actual speed, actual speed averaged, current draw, and average current draw (Maxon®, 2021). By extending wires directly from the hall sensor pins on the motor controller, it allows you to directly read the position of the motor using data from tics of the motor, which can later be converted into an angle, and manipulated from that.

The motor controllers in this configuration are set up to receive a high or low input from the Arduino controller which will enable the motor to spin, and then will in turn receive an analog signal on a range of 0 to 5 Volts that will control the speed range from -500 to 500 rpm.

Figure 48: The Maxon® ESCON 50/5, 4-Q Servo controller for DC/EC motors, 5/15 A, 10 - 50 VDC

ESCON® Studio

The motor controller is controlled through the proprietary ESCON® Studio software provided with the product. In this software, the user may test their motor, and configure it in any way they need for their particular application. Also, the software offers a tuning service where you may tune the motor specifications to real world application to make them even more accurate.

In this scenario, we chose from a list of control methods to control our motors through a closed-loop speed control situation where the motor controller would receive a signal from the Arduino on a range of 0 to 5 Volts that was directly correlated with desired speed. As mentioned above, after tuning this system rigorously we settled on the operating range of -500 to 500 rpm for minimum and maximum speed. The software also allows the user to implement an acceleration and deceleration ramp in order to make operation much smoother (Maxon®, 2021). The ramp that was decided upon in the final iteration of the testing process was 4000 rev/min/s^2 which allowed for a natural gait cycle in approaching the desired angles as determined by the potentiometers.

Future Recommendations

Through the creation of this smart military exoskeleton, there were many successful milestones that were reached. The prototype was able to be manufactured and assembled, perfectly fitting the test patient. The correct walking gait cycle was able to be programmed into the exoskeleton to assist with walking. If this project was to continue, there is a set of recommendations that would take this project to the next level.

The first recommendation would be to use cloud-based CAD software like Fusion 360® over locally stored CAD programs like SolidWorks®. This would streamline the CAD creation/editing process significantly allowing multiple team members to contribute simultaneously. Fusion 360® is also compatible with Windows®, macOS®, and web browsers, with simplified applications available for Android® and iOS®.

Regarding the hardware of the exoskeleton, our suggestion would be to anodize the clutches after manufacturing them. This would strengthen the aluminum and not allow for the D-shaft to mold it through when excessive torque is produced. Since the D-shaft used was made from stainless steel, it was able to deform D-shaped slot in the clutch which, therefore, causing setbacks in the clutch engagement. Anodized aluminum clutches would fix this problem.

To continue, a further recommendation would be to use stronger and harder steel for the plates along the lower body extremities of the user. The use of non hardened A-36 steel left the exoskeleton weaker than desired. The tibia and femur plates both bent slightly, and the hip plates were initially torn through by the stainless steel D-shaft. With the use of a high strength and hardened steel, the plates would not be as susceptible to bending and the D-shaft would not be able to rotate internally within the hip parts no matter the initial tolerancing.

Another suggestion would be to use springs that are better rated for our desired torque and that are also lighter. The springs that are used are created for truck bed movement, so they are very high in torque and also rather heavy. With a larger budget, better springs could be purchased that would be more compact, lighter weight and better fit for this specific torque application.

In terms of electronic components of the exoskeleton, our recommendation would be the use of a higher bias on sensor input to make this exoskeleton more electronically sophisticated. In early iterations our goal was to affect each step based on sensor input from strain gauges. This would allow the exoskeleton to walk with the user based on how much force was being exerted on each step, allowing for variability in each step considering no gait cycle is the same every time.

Another suggestion for controls part of this project would be the use of kinematics in the gait cycle to calculate the acceleration of the end effector (in this case the foot) to tell how fast the person was walking. In combination with load cells, kinematics could be actively calculated during each step in combination with a load cell on the bottom of the foot to be able to tell when the foot was on the ground. From this, you could perform inverse kinematics in order to tell where hip and knee positions are, and how fast the leg in its entirety is moving.

The last recommendation would be to implement brushless stepper motors to replace the current flat brushless DC motors. These would provide better controls to be implemented in the coding, allowing them to turn to more specific angles. This could create more customizable movements adjusted for a specific user.

In order to evaluate whether the developed exoskeleton can fulfill its main function of decreasing the metabolic cost of movement, our team has developed a detailed protocol to evaluate the energy expenditure before and after the use of the exoskeleton. Mentioned protocol consists of two experiments that should be ran simultaneously to guarantee the proper data collection and verify the collected result. The “golden standard” for the measurement of metabolic costs is Indirect Calorimetry (IC) (Delsoglio, 2019). This test is based on the mathematical formula that approximates the amount of calories consumed during a certain period of time by considering the pulmonary gas exchanges. Mathematical formula used was chosen to be Weir’s equation that can be expressed as:

Kcal used = [(V(O2) × 3.941) + (V(CO2) × 1.11)] × 1440), where the V(O2) represents the amount of oxygen inhaled and V(CO2) is the amount of CO2 exhaled (Delsoglio, 2019).

In the case of this project, an “open circuit systems” test should be used (Mtaweh, 2018). To measure oxygen consumption, a direct spirometer, and Logger Pro® 3 software (Vernier, USA) should be used.

The other test was chosen to be the Physiological Cost Index (PCI). PCI is an abstract mathematical tool that indirectly assesses oxygen consumption during certain activity with the energy cost of this activity. It is evaluated by considering the heart rate in relation to the speed. The formula used to calculate PCI is "walking heart rate minus resting heart rate divided by speed" (Karami et al., 2020). Pulse oximeter sensor is meant to be used to collect data on the heart rate throughout the test.

Described tests had to be executed on three different days but following the same environmental conditions (fatigue level, eating and sleeping schedule, etc.). The table in Appendix C contains the parameters for the physical tests to follow. The activity described in Appendix C should be performed with and without an exoskeleton for evaluation purposes.

The data collected from the described test should be analyzed to evaluate the exoskeleton's effectiveness in performance enhancing.

Broader Impact

A.1 Engineering Ethics

This intelligent exoskeleton suit was created in accordance with the Mechanical Engineering Code of Ethics. The significance of upholding a high standard of professionalism, integrity, and responsibility in their work is emphasized by the ethical principles for mechanical engineers.

The main objective of the device is to increase the efficiency and effectiveness of soldiers by giving them the assistance they need and lowering their risk of harm from carrying heavy weights. By protecting the health and welfare of soldiers who defend their nation, this design serves society.

Second, sustainability and environmental responsibility were the main tenets of our design strategy. We made use of materials that are strong, light, and healthy for the environment. By adopting sustainable design practices, we are not only reducing our environmental footprint but also contributing to the long-term sustainability of our society.

Thirdly, we made steps to guarantee the dependability and safety of our product. We performed rigorous testing on the leg movement to make sure the motors wouldn't operate improperly and harm the user. A mechanical safety stop was added to prevent the user's legs from bending at an uncomfortable angle, and an E-stop button was added to stop the motor's rotation.

Fourth, we followed ethical guidelines for intellectual property, making sure that all of our designs, and inventions are original to us. Additionally, we avoided violating any already-existing patents, trademarks, or copyrights. We adhere to the moral standard of upholding honesty and professionalism by protecting intellectual property rights.

In conclusion, the creation of an intelligent exoskeleton suit that would decrease fatigue in soldiers who are carrying high loads is in line with the Mechanical Engineering Code of Ethics. Our product puts a priority on safety and dependability, encourages sustainability and environmental responsibility, and upholds intellectual property rights. We are happy to have made a social contribution while upholding the highest moral standards as students who planned and produced this product.

A.2 Societal and Global Impact

There could be a variety of effects on both individuals and groups of people from the creation of a smart exoskeleton suit meant to lessen troop fatigue. The primary objective of the suit is to improve soldiers' physical performance in combat, which may have both intentional and unforeseen effects on users and other stakeholders.

From a health standpoint, the smart exoskeleton suit may lessen the possibility of harm or stress on the body brought on by carrying heavy objects for extended periods of time. The suit may distribute the weight of the equipment so that soldiers can carry it more easily without putting undue strain on their muscles and joints. This might lessen musculoskeletal injuries and enhance the general physical health of soldiers. Exoskeleton has the potential to be overused, which could result in a decline in natural physical fitness and a higher risk of injury when not wearing the suit. This won't happen unless more users start wearing the suit daily.

The exoskeleton suit could improve troops' safety by enabling them to perform better in hazardous conditions. A soldier's speed and power might be increased by the suit, enabling them to endure riskier and harder engagements. Increased overconfidence, on the other hand, runs the risk of encouraging riskier behavior and a delusion of invincibility.

The effect of the exoskeleton suit on civilian populations may be another unexpected consequence. It could be utilized to help the elderly or those with physically demanding jobs. These communities might experience a substantial change as a result, perhaps resulting in fewer work-related accidents and higher quality of life.

In conclusion, the development of a smart exoskeleton suit designed to reduce soldier fatigue has the potential to impact individuals and groups in various ways. While there are potential benefits to the suit, such as improved health, safety, and welfare of soldiers, there are also unintended consequences to consider, such as overreliance on technology.

A.3 Environmental Impact

The smart exoskeleton designed to reduce soldier fatigue has the potential to impact the environment in several ways, both intended and unintended. The product was built using carbon fiber molds and aluminum manufacturing, which both have environmental implications.

One of the intended consequences of the exoskeleton's design is to reduce the physical fatigue of soldiers, which can lead to improved operational effectiveness and safety. By reducing the physical burden on soldiers, the exoskeleton can also reduce the risk of injury, which can have long-term sustainability benefits. This improvement could create less of a reliance on healthcare for many veterans. It could also increase veteran morale as they will hopefully have less injuries after leaving the military.

However, the production of carbon fiber molds and aluminum components has environmental implications. Carbon fiber production is energy-intensive and requires significant amounts of electricity, which can lead to increased greenhouse gas emissions. The manufacturing of aluminum stock requires significant energy and can cause pollution both in water and air. The energy used for this manufacturing process can create unnecessary greenhouse gases.

The exoskeleton uses a 58-volt battery and four motors, which may also have environmental impacts. The production and disposal of batteries can be harmful to the environment due to the materials used in their construction, such as heavy metals. The motors also require electricity to function, which more greenhouse gas emissions and further fossil fuel consumption.

Furthermore, the disposal of the exoskeleton at the end of its lifecycle can also have unintended consequences. The carbon fiber and aluminum components are not biodegradable so they will end up in landfills which highly contribute to pollution and waste.

In conclusion, the student group's smart exoskeleton designed to reduce soldier fatigue has the potential to impact the environment in several ways, both intended and unintended. While the exoskeleton may have positive benefits for soldier health and safety, it is important to consider the environmental implications of its design, production, use, and disposal. It is essential to conduct a life-

cycle assessment to minimize the environmental impact of the product and identify opportunities for sustainable design and manufacturing practices.

A.4 Codes and Standards

The development of a smart exoskeleton suit involves adhering to several technical codes and standards to ensure its safe and effective use. One of the most critical standards to consider is the ISO 13482:2014, which outlines the safety requirements for personal care robots. This standard sets guidelines for the design, manufacturing, and use of robots that interact with people, including exoskeletons. Complying with this standard ensures that the suit is safe to use and will not harm the user or anybody around them.

Another essential standard to follow is the ISO 10218:2011, which specifies the safety requirements for industrial robots. This standard encompasses the design and manufacturing of the robot, along with the operation and maintenance of it. The standard outlines the requirements for the control systems, power sources, and emergency stop functions, among other critical aspects. By following this standard, we can ensure that the exoskeleton suit is safe, reliable, and efficient.

Additionally, we need to follow specific technical codes and standards for materials, software, and hardware used in the exoskeleton suit. For example, the use of high strength and durable materials is needed to ensure the longevity of the product. The software and hardware used in the exoskeleton suit must also be designed to integrate seamlessly and reliably with the suit's mechanical components. Overall, adherence to these technical codes and standards is crucial for the development of a safe and effective smart exoskeleton suit used to reduce fatigue.

A.5 Economic Factors

There are several economic factors that may be driving the development and production of our smart exoskeleton suit that costs $1,800 to build, as well as influencing its pricing and market competition.

The advancements in technology, such as the development of sensors, motors, and lightweight materials, have enabled the creation of smart exoskeleton suits that are affordable to manufacture. These technological advancements have also led to increased efficiency, safety, and durability, which may drive demand for these suits in various industries.

The cost of labor plays a significant role in determining the cost of production of smart exoskeleton suits. Due to the increase in automation across the manufacturing industry, the labor cost is decreasing. This will allow the suits to be sold for a competitive price compared to other suits.

There may be a growing demand for smart exoskeleton suits in various industries, such as construction, manufacturing, and healthcare. The increasing demand for these suits may drive the competition in the market, leading to more affordable pricing for consumers. The competition in the market may also lead to price wars, which can lower the cost .

The cost of research and development for smart exoskeleton suits may also impact the final cost of production and pricing for consumers. The investment in research and development may increase the cost of design, which may lead to a higher price tag.

In conclusion, several economic factors influence the production, pricing, and competition of smart exoskeleton suits. The technological advancements, cost of labor, market demand, competition, and research and development costs all play a role in determining the final cost to consumers and competitiveness in the market.

Conclusion

This exoskeleton was highly successful for being a first-round prototype. The fitment of the exoskeleton on our test patient was perfect, which was one of the main goals for the design aspect. Due to the difficulty of the design and manufacturing phases, not all the initial goals were able to be met. Although this may seem like a failure, the overall project was a success because of the final assembled product. It is important to remember that this product is an initial prototype that will be further developed and improved on in a future project. The strides made throughout this year will successfully set up a future project to be able to further develop a functioning army exoskeleton. With the advancements made, future groups will be able to focus on material selection, coding and sensing that will bring this exoskeleton to the next level.

Appendix

Appendix A: Bill of Materials

Part	Quantity	Material
Foot		
Heel Cup	2	Carbon fiber
Boot Lock	2	PETG
Foot Side Plates	4	A36 steel
Ankle Cup	2	Carbon fiber
Ankle Side Plates	4	A36 steel
Potentiometer Gear Mount	2	PLA
Short Velcro Strap	2	Velcro
Leg		
Spline	2	Carbon Fiber
Spline/Ankle 1/2" ID Bushing	2	brass
Tibia Plate	2	A36 steel
Alumnium Angle	6	6061 Aluminum
Spring Engager	2	PLA
Knee Mechanical Stop	2	A36 steel
Inner Knee Plate	2	A36 steel
Femur Plate	2	A36 steel
Knee-Shaft 3/8" ID Bushing	2	brass
Spacer Plates	2	PLA
Rotating Hip Plate	2	A36 steel
Surface-Mount Hinge	2	316 Stainless Steel
Long Velcro Straps	6	Velcro
Hip/Lower Back		
Hip Mount Plate	2	A36 steel
Hip Mount	2	6061 Aluminum
Spacer Plates	2	PLA
Lower Back Plate	2	A36 steel

4" Hex Standoff	8	Aluminum
Harness	1	Polyester/Nylon
Lower Back Mounts	2	PLA
2" Round Coupling Nut	2	Black oxide steel
Battery Box/Sensors		
Box	1	Birch
50A Motor Controllers	2	N/A
70A Moter Controllers	2	N/A
Motor Controller Housing	4	PLA
Arduino Mega	1	
Breadboard	1	
Potentiometers	4	
Potentiometer Mounts	4	PLA
Gearbox (x4)		
Clutch	2	6061 aluminum
Maxon Motor	1	N/A
Clutch Engager	2	PLA
Stacked Wave Disc Spring	2	High Carbon Steel
5/8" ID Bushing	2	Brass
Standoff	4	6061 Aluminum
Spiral Spring	2	High Carbon Steel
Spring Insert	1	PLA
Spring Insert Pins 1/4" Diameter	2	Low carbon Steel
Gearbox Housing Plate	2	A36 steel
Gearbox Housing cover	1	PLA
Square Gear Shafts	2	A36 steel
Top 5/8" D shaft	1	Stainless Steel
Bottom 5/8" D shaft	1	Stainless Steel
3/8" ID Flange bearing	5	Chrome Steel
96 Tooth Gear	2	A36 steel
76 Tooth Gear	1	A36 steel
19 Tooth Gear	2	A36 steel

Light Duty Thrust Washers 5/8” ID	2	Thermoplastic blend
Gear Standoff	1	PLA
External Retaining Ring 5/8" OD	1	1060 Steel
Fasteners		
1/2"-(10/32) Hex head steel screws	28	Grade 8 steel
3/8"-16 x 5" Steel screws	2	Grade 5 steel
1/2"-13 High strength lock nut	2	High strength steel
1/2"-13 x 2.5" Flat head screw	2	Alloy steel
3/8"-16 x 1.25” Flat head screw	12	Alloy steel
3/8"-16 Nylon insert lock nut	14	High strength steel
5/16"-18 x 1” Slotted Flat head screw	6	Stainless steel
5/16"-18 Steel hex nuts	6	Grade 5 steel
1/4"-20 High strength lock nut	50	High strength steel
1/4"-20 x 1.5" Flat head screw	8	Alloy Steel
1/4"-20 x 3" Hex head screw	8	Alloy Steel
1/4"-20 x 2.75" Hex head screw	10	Alloy Steel
1/4"-20 x 4.5" Hex head screw	8	Alloy Steel
Washer 1/4" ID	2	Alloy Steel
1/4"-20 x 0.75" Hex head screw	12	Alloy Steel
1/8"-20 x 0.5" Flat head screw	8	Alloy Steel
1/8"-20 x 0.5" threaded screw insert	8	Alloy Steel

Appendix B: Programming Code

```
// all I/O pins corresponding to the arduino wiring
#define estop 13

#define enable_r_hip 12
#define sped_r_hip 11
#define enable_r_knee 9
#define sped_r_knee 8

#define enable_l_hip 7
#define sped_l_hip 6
#define enable_l_knee 4
#define sped_l_knee 3

#define r_hip_pot_pin A0
#define r_knee_pot_pin A1
#define l_hip_pot_pin A2
#define l_knee_pot_pin A3

// ration to convert potentiometer readings to degree measurements
double pot_to_angle = 300.0 / 1024.0;

// value range in degrees to determine if motors are at desired position
int target_threshold = 3;

// initial starting direction for right leg
bool r_hip_forward = true;
bool r_knee_forward = true;

// initial starting direction for left leg
bool l_hip_forward = false;
bool l_knee_forward = false;

// initializing leg variables
int r_hip_initial = 0;
int r_knee_initial = 0;
double r_desired_hip_angle = 0;
double r_desired_knee_angle = 0;
double r_hip_angle = 0.0;
double r_knee_angle = 0.0;
double r_hip_error = 0.0;
double r_knee_error = 0.0;
double r_prev_hip_error = 0.0;
double r_prev_knee_error = 0.0;
double r_hip_Kp = 0.0;
double r_hip_Kd = 0.0;
double r_knee_Kp = 0.0;
double r_knee_Kd = 0.0;

int l_hip_initial = 0;
int l_knee_initial = 0;
double l_desired_hip_angle = 0;
double l_desired_knee_angle = 0;
double l_hip_angle = 0.0;
double l_knee_angle = 0.0;
double l_hip_error = 0.0;
double l_knee_error = 0.0;
double l_prev_hip_error = 0.0;
double l_prev_knee_error = 0.0;
double l_hip_Kp = 0.0;
double l_hip_Kd = 0.0;
double l_knee_Kp = 0.0;
double l_knee_Kd = 0.0;

// assigned P and D values for legs moving both forward and backward
double forward_r_hip_Kp = 0.4;
double forward_r_hip_Kd = 6.0;
double backward_r_hip_Kp = 0.15;
double backward_r_hip_Kd = 4.0;
double forward_r_knee_Kp = 0.3;
double forward_r_knee_Kd = 6.0;
double backward_r_knee_Kp = 0.2;
```

```
double backward_r_knee_Kd = 5.0;

double forward_l_hip_Kp = 0.4;
double forward_l_hip_Kd = 6.0;
double backward_l_hip_Kp = 0.15;
double backward_l_hip_Kd = 4.0;
double forward_l_knee_Kp = 0.3;
double forward_l_knee_Kd = 6.0;
double backward_l_knee_Kp = 0.2;
double backward_l_knee_Kd = 5.0;

// desired forward and backward angles for legs in gait cycle
double forward_hip_angle = 25.0;
double backward_hip_angle = -5.0;
double forward_knee_angle = 0.0;
double backward_knee_angle = -20.0;


void setup() {

  // setup and assignment of all I/O pins
  pinMode(estop, INPUT);
  digitalWrite(estop, LOW);

  pinMode(enable_r_hip, OUTPUT);
  pinMode(sped_r_hip, OUTPUT);
  pinMode(enable_r_knee, OUTPUT);
  pinMode(sped_r_knee, OUTPUT);
  pinMode(enable_l_hip, OUTPUT);
  pinMode(sped_l_hip, OUTPUT);
  pinMode(enable_l_knee, OUTPUT);
  pinMode(sped_l_knee, OUTPUT);

  digitalWrite(enable_r_hip, LOW);
  digitalWrite(enable_r_knee, LOW);
  digitalWrite(enable_l_hip, LOW);
  digitalWrite(enable_l_knee, LOW);

  pinMode(r_hip_pot_pin, INPUT);
  pinMode(r_knee_pot_pin, INPUT);
  pinMode(l_hip_pot_pin, INPUT);
  pinMode(l_knee_pot_pin, INPUT);

  // getting potentiometer readings on startup to zero them out
  r_hip_initial = analogRead(r_hip_pot_pin);
  r_knee_initial = analogRead(r_knee_pot_pin);
  l_hip_initial = analogRead(l_hip_pot_pin);
  l_knee_initial = analogRead(l_knee_pot_pin);

  Serial.begin(9600);
}

// all code to be executed continuously
void loop() {

  check_estop();

  r_hip_calculations();
  r_knee_calculations();
  l_hip_calculations();
  l_knee_calculations();

  r_hip_control();
  r_knee_control();
  l_hip_control();
  l_knee_control();
  }

/*  next four functions perform all calculations for each motor including:
 *    zeroed out potentiometer reading
 *    actual angle reading assuming it is initialized with straight legs
 *    error in actual angle and and current desired angle
 *    checking if both motors for that leg are at their designated position
 *    setting desired motor direction if leg within threshold
 *    setting desired motor angle depending on motor direction
```

```
 *    setting desired P and D values depending on motor direction
 */
void r_hip_calculations() {

  int hip_pot_reading = analogRead(r_hip_pot_pin) - r_hip_initial;
  r_hip_angle = hip_pot_reading * pot_to_angle;

  r_hip_error = r_hip_angle - r_desired_hip_angle;

  if (abs(r_hip_angle - forward_hip_angle) < target_threshold &&
      abs(r_knee_angle - forward_knee_angle) < target_threshold) {
    r_hip_forward = false;
  }
  else if (abs(r_hip_angle - backward_hip_angle) < target_threshold &&
      abs(r_knee_angle - backward_knee_angle) < target_threshold) {
    r_hip_forward = true;
  }

  if (r_hip_forward) {
    r_desired_hip_angle = forward_hip_angle;
    r_hip_Kp = forward_r_hip_Kp;
    r_hip_Kd = forward_r_hip_Kd;
  }
  else{
    r_desired_hip_angle = backward_hip_angle;
    r_hip_Kp = backward_r_hip_Kp;
    r_hip_Kd = backward_r_hip_Kd;
  }
}

void r_knee_calculations() {

  int knee_pot_reading = analogRead(r_knee_pot_pin) - r_knee_initial;
  r_knee_angle = knee_pot_reading * pot_to_angle;

  r_knee_error = r_knee_angle - r_desired_knee_angle;

  if (abs(r_knee_angle - forward_knee_angle) < target_threshold &&
      abs(r_hip_angle - forward_hip_angle) < target_threshold) {
    r_knee_forward = false;
  }
  else if (abs(r_knee_angle - backward_knee_angle) < target_threshold &&
      abs(r_hip_angle - backward_hip_angle) < target_threshold) {
    r_knee_forward = true;
  }

  if (r_knee_forward) {
    r_desired_knee_angle = forward_knee_angle;
    r_knee_Kp = forward_r_knee_Kp;
    r_knee_Kd = forward_r_knee_Kd;
  }
  else{
    r_desired_knee_angle = backward_knee_angle;
    r_knee_Kp = backward_r_knee_Kp;
    r_knee_Kd = backward_r_knee_Kd;
  }
}

void l_hip_calculations() {

  int hip_pot_reading = analogRead(l_hip_pot_pin) - l_hip_initial;
  l_hip_angle = hip_pot_reading * pot_to_angle;

  l_hip_error = l_hip_angle - l_desired_hip_angle;

  if (abs(l_hip_angle - forward_hip_angle) < target_threshold &&
      abs(l_knee_angle - forward_knee_angle) < target_threshold) {
    l_hip_forward = false;
  }
  else if (abs(l_hip_angle - backward_hip_angle) < target_threshold &&
      abs(l_knee_angle - backward_knee_angle) < target_threshold) {
    l_hip_forward = true;
  }

  if (l_hip_forward) {
```

```
    l_desired_hip_angle = forward_hip_angle;
    l_hip_Kp = forward_l_hip_Kp;
    l_hip_Kd = forward_l_hip_Kd;
  }
  else{
    l_desired_hip_angle = backward_hip_angle;
    l_hip_Kp = backward_l_hip_Kp;
    l_hip_Kd = backward_l_hip_Kd;
  }
}

void l_knee_calculations() {

  int knee_pot_reading = analogRead(l_knee_pot_pin) - l_knee_initial;
  l_knee_angle = knee_pot_reading * pot_to_angle;

  l_knee_error = l_knee_angle - l_desired_knee_angle;

  if (abs(l_knee_angle - forward_knee_angle) < target_threshold &&
      abs(l_hip_angle - forward_hip_angle) < target_threshold) {
    l_knee_forward = false;
  }
  else if (abs(l_knee_angle - backward_knee_angle) < target_threshold &&
      abs(l_hip_angle - backward_hip_angle) < target_threshold) {
    l_knee_forward = true;
  }

  if (l_knee_forward) {
    l_desired_knee_angle = forward_knee_angle;
    l_knee_Kp = forward_l_knee_Kp;
    l_knee_Kd = forward_l_knee_Kd;
  }
  else{
    l_desired_knee_angle = backward_knee_angle;
    l_knee_Kp = backward_l_knee_Kp;
    l_knee_Kd = backward_l_knee_Kd;
  }
}

/*  next four functions handle the PD control including:
 *    calculating the needed PD output given the set variables and errors
 *    resetting the previous error
 *    capping the calculated PD output to a range of -60 to 60
 *    calling the move motor function
 */
void r_hip_control() {

  double pid_out = r_hip_error * r_hip_Kp + r_hip_Kd * (r_hip_error - r_prev_hip_error);
  r_prev_hip_error = r_hip_error;

  if (pid_out > 0){
    if (pid_out > 60){
      pid_out = 60;
    }
  }
  else {
    if (pid_out < -60){
      pid_out = -60;
    }
  }

  r_hip_motor_move(pid_out);
}

void r_knee_control() {

  double pid_out = r_knee_error * r_knee_Kp + r_knee_Kd * (r_knee_error - r_prev_knee_error);
  r_prev_knee_error = r_knee_error;

  if (pid_out > 0){
    if (pid_out > 60){
      pid_out = 60;
    }
  }
  else {
```

```
    if (pid_out < -60){
      pid_out = -60;
    }
  }

  r_knee_motor_move(pid_out);
}

void l_hip_control() {

  double pid_out = l_hip_error * l_hip_Kp + l_hip_Kd * (l_hip_error - l_prev_hip_error);
  l_prev_hip_error = l_hip_error;

  if (pid_out > 0){
    if (pid_out > 60){
      pid_out = 60;
    }
  }
  else {
    if (pid_out < -60){
      pid_out = -60;
    }
  }

  l_hip_motor_move(pid_out);
}

void l_knee_control() {

  double pid_out = l_knee_error * l_knee_Kp + l_knee_Kd * (l_knee_error - l_prev_knee_error);
  l_prev_knee_error = l_knee_error;

  if (pid_out > 0){
    if (pid_out > 60){
      pid_out = 60;
    }
  }
  else {
    if (pid_out < -60){
      pid_out = -60;
    }
  }

  l_knee_motor_move(pid_out);
}

/*  next four functions handle outputting to the motor controllers including:
 *    remapping the PD output from -60 - 60 to 0 - 255 for the desired speed
 *    sending the mapped value to the designated motor controller
 */
void r_hip_motor_move(double spd){

  double out = map(spd, -60, 60, 0, 255);
  analogWrite(sped_r_hip, out);
}

void r_knee_motor_move(double spd){

  double out = map(spd, -60, 60, 0, 255);
  analogWrite(sped_r_knee, out);
}

void l_hip_motor_move(double spd){

  double out = map(spd, -60, 60, 255, 0);
  analogWrite(sped_l_hip, out);
}

void l_knee_motor_move(double spd){

  double out = map(spd, -60, 60, 255, 0);
  analogWrite(sped_l_knee, out);
}

// handles the estop button checking if it is pressed to disable all motors
```

```
void check_estop() {

  if (digitalRead(estop)) {
    digitalWrite(enable_r_hip, LOW);
    digitalWrite(enable_r_knee, LOW);
    digitalWrite(enable_l_hip, LOW);
    digitalWrite(enable_l_knee, LOW);
    }
}
```

Appendix C: Testing Protocol Table

Activity	**Testing Parameter**			
	Added mass (lbs)	***Speed (mi/h)***	***Exercise time (min)***	***Resting time (min)***
Treadmill	0	2.5	3	3
	60	1.8	3	5
Stepmill	0	1.5	3	4
	60	0.9	3	6

Appendix D: Final Assembly Documentation

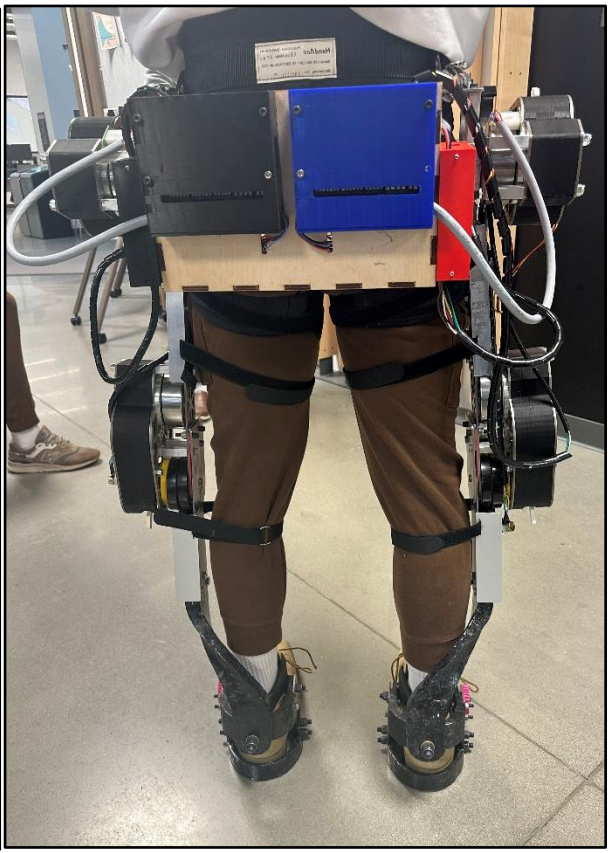

References

1. *All About Force Sensors - Types and How They Work*. (n.d.). Thomasnet. Retrieved October 24, 2022, from https://www.thomasnet.com/articles/instruments-controls/all-about-force-sensors/
2. Anderson, M. (2019, June 10). *What is the Difference Between Absolute and Incremental Encoders?* RealPars. Retrieved October 24, 2022, from https://realpars.com/absolute-vs-incremental-encoder/
3. Battery Comparison of Energy Density - Cylindrical and Prismatic Cells. (n.d.). Epec Engineered Technologies. Retrieved October 24, 2022, from https://www.epectec.com/batteries/cell-comparison.html
4. Benn ML, Pizzari T, Rath L, Tucker K, Semciw AI. Adductor magnus: An EMG investigation into proximal and distal portions and direction specific action. Clin Anat. 2018 May;31(4):535-543. doi: 10.1002/ca.23068. Epub 2018 Mar 23. PMID: 29520841.
5. Binstead JT, Munjal A, Varacallo M. Anatomy, Bony Pelvis and Lower Limb, Calf. [Updated 2022 May 29]. In: StatPearls [Internet]. Treasure Island (FL): StatPearls Publishing; 2022 Jan-. Available from: https://www.ncbi.nlm.nih.gov/books/NBK459362/
6. Biondi NL, Varacallo M. Anatomy, Bony Pelvis and Lower Limb, Vastus Lateralis Muscle. [Updated 2021 Aug 13]. In: StatPearls [Internet]. Treasure Island (FL): StatPearls Publishing; 2022 Jan-. Available from: https://www.ncbi.nlm.nih.gov/books/NBK532309/
7. Bordoni B, Varacallo M. Anatomy, Bony Pelvis and Lower Limb, Thigh Quadriceps Muscle. [Updated 2022 May 10]. In: StatPearls [Internet]. Treasure Island (FL): StatPearls Publishing; 2022 Jan-. Available from: https://www.ncbi.nlm.nih.gov/books/NBK513334/
8. Delsoglio, M., Achamrah, N., Berger, M. M., & Pichard, C. (2019). Indirect calorimetry in clinical practice. Journal of Clinical Medicine, 8(9), 1387. https://doi.org/10.3390/jcm8091387
9. Department of Army Headquarters. (2022, April). Foot Marches. Retrieved September 25, 2022, from https://irp.fas.org/doddir/army/atp3-21-18.pdf
10. Elzanie A, Borger J. Anatomy, Bony Pelvis and Lower Limb, Gluteus Maximus Muscle. [Updated 2022 Mar 28]. In: StatPearls [Internet]. Treasure Island (FL): StatPearls Publishing; 2022 Jan-. Available from: https://www.ncbi.nlm.nih.gov/books/NBK538193/
11. Fox, S., Aranko, O., Heilala, J., & Vahala , P. (2019, June 17). Exoskeletons: Comprehensive, comparative and critical analyses of their potential to improve manufacturing performance. Emerald Insight. Retrieved September 29, 2022, from https://www.emerald.com/insight/content/doi/10.1108/JMTM-01-2019-0023/full/html#sec07

12. Glenister R, Sharma S. Anatomy, Bony Pelvis and Lower Limb, Hip. [Updated 2021 Jul 26]. In: StatPearls [Internet]. Treasure Island (FL): StatPearls Publishing; 2022 Jan-. Available from: https://www.ncbi.nlm.nih.gov/books/NBK526019/
13. Gold M, Munjal A, Varacallo M. Anatomy, Bony Pelvis and Lower Limb, Hip Joint. [Updated 2021 Jul 31]. In: StatPearls [Internet]. Treasure Island (FL): StatPearls Publishing; 2022 Jan-. Available from: https://www.ncbi.nlm.nih.gov/books/NBK470555/
14. Greco AJ, Vilella RC. Anatomy, Bony Pelvis and Lower Limb, Gluteus Minimus Muscle. [Updated 2022 May 29]. In: StatPearls [Internet]. Treasure Island (FL): StatPearls Publishing; 2022 Jan-. Available from: https://www.ncbi.nlm.nih.gov/books/NBK556144/
15. Hersum, A., Ferrua Elmudesi, R., Waterman, J., Habboosh, D., & Chapins, Z. (2022). Autonomous Exoskeleton for Paraplegic Assistance. : Worcester Polytechnic Institute.
16. Huang, L., Yang, Z., Wang, R., & Xie, L. (2020, June 13). Physiological and biomechanical effects on the human musculoskeletal system while carrying a suspended-load backpack. Science Direct. Retrieved September 24, 2022, from https://www.sciencedirect.com/science/article/pii/S0021929020303171
17. Hemmes, K., & Bakker, S. (2019, October 10). *Sensors for speed measurements — Istec*. Istec International. Retrieved October 24, 2022, from https://www.istec.com/en/sensors-for-speed-measurements/
18. Husseini, Talal, and Talal Husseini. “US Army Trials Exoskeletons for Military Use.” Army Technology, 11 June 2020, https://www.army-technology.com/analysis/us-army-exoskeletons/.
19. Jackson , K. (2021). Walking - Muscles Used. Physiopedia. Retrieved October 7, 2022, from https://www.physio-pedia.com/Walking_-_Muscles_Used
20. Jeno SH, Schindler GS. Anatomy, Bony Pelvis and Lower Limb, Thigh Adductor Magnus Muscle. [Updated 2021 Aug 8]. In: StatPearls [Internet]. Treasure Island (FL): StatPearls Publishing; 2022 Jan-. Available from: https://www.ncbi.nlm.nih.gov/books/NBK534842/
21. Karami H, Karami K, Abdullatif Khafaie M, Zahednejad S, Arastoo AA. The Physiological Cost Index and Some Kinematic Parameters of Walking and Jogging in Blind and Sighted Students. Iran J Med Sci. 2020 Jan;45(1):16-22. doi: 10.30476/ijms.2019.45386. PMID: 32038055; PMCID: PMC6983280.
22. Kim SM, Yoo WG. Comparison of trunk and hip muscle activity during different degrees of lumbar and hip extension. J Phys Ther Sci. 2015 Sep;27(9):2717-8. doi: 10.1589/jpts.27.2717. Epub 2015 Sep 30. PMID: 26504276; PMCID: PMC4616077.
23. Krishna. “Raytheon XOS 2 Exoskeleton, Second-Generation Robotics Suit.” Army Technology, Verdict, 11 June 2020, https://www.army-technology.com/projects/raytheon-xos-2-exoskeleton-us/.

24. Laschowski, B., McPhee, J., and Andrysek, J. (May 17, 2019). "Lower-Limb Prostheses and Exoskeletons With Energy Regeneration: Mechatronic Design and Optimization Review." ASME. J. Mechanisms Robotics. August 2019; 11(4): 040801. https://doi-org.ezpv7-web-p-u01.wpi.edu/10.1115/1.4043460
25. “LegX.” Suitx, https://www.suitx.com/legx.
26. Lithium-Ion Battery - Clean Energy Institute. (n.d.). Clean Energy Institute. Retrieved October 24, 2022, from https://www.cei.washington.edu/education/science-of-solar/battery-technology/
27. Liu, M. Q., Anderson, F. C., Pandy, M. G., & Delp, S. L. (2005, October 10). Muscles that support the body also modulate forward progression during walking. Journal of Biomechanics. Retrieved October 8, 2022, from https://www.sciencedirect.com/science/article/pii/S0021929005003970?via%3Dihub
28. LockheedMartin. Take a Step into the Future with ONYX. YouTube, YouTube, 25 Feb. 2019, https://www.youtube.com/watch?v=U6VlXHuMNXE. Accessed 13 Sept. 2022.
29. Marinov, Bobby, et al. “19 Military Exoskeletons into 5 Categories.” Exoskeleton Report, 9 Sept. 2019, https://exoskeletonreport.com/2016/07/military-exoskeletons/.
30. Maxwell, Keith. Lockheed Martin Exhibits ONYX Exoskeleton at AUSA. YouTube, YouTube, 16 Oct. 2019, https://www.youtube.com/watch?v=o4Llz1Gy7Lg. Accessed 13 Sept. 2022.
31. *Motor Encoder Speed & Position Overview | Dynapar*. (n.d.). Dynapar Encoders. Retrieved October 24, 2022, from https://www.dynapar.com/technology/encoder_basics/motor_encoders/
32. Mittal, Vikram. “Why Military Exoskeletons Will Remain Science Fiction.” Forbes, Forbes Magazine, 18 Aug. 2020, https://www.forbes.com/sites/vikrammittal/2020/08/17/military-exoskeletons-science-fiction-or-science-reality/?sh=37e7128ba69e.
33. *MILE Encoder for EC 90 flat / Product Information*. (n.d.). maxon Group. Retrieved October 24, 2022, from https://www.maxongroup.com/medias/sys_master/8814678704158.pdf
34. Mtaweh, H., Tuira, L., Floh, A. A., & Parshuram, C. S. (2018). Indirect calorimetry: History, technology, and application. *Frontiers in Pediatrics, 6*. https://doi.org/10.3389/fped.2018.00257
35. *MyoWare 2.0 Muscle Sensor - DEV-18977*. (n.d.). SparkFun Electronics. Retrieved October 24, 2022, from https://www.sparkfun.com/products/18977
36. Orr, R. M., Johnston , V., Pope, R., & Coyle, J. (2013, September 13). Soldier occupational load carriage: a narrative review of associated injuries. Taylor & Francis Online. Retrieved September 23, 2022, from https://doi-org.ezpv7-web-p-u01.wpi.edu/10.1080/17457300.2013.833944

37. *Raytheon Xos-2 Exoskeleton*. (2020). Army Technology. Retrieved September 2022, from https://www.army-technology.com/projects/raytheon-xos-2-exoskeleton-us/.
38. Rechargeable Batteries Guide | NiMH | Li-ion | NiCd. (n.d.). Microbattery. Retrieved October 24, 2022, from https://www.microbattery.com/rechargeable-batteries-guide
39. Rodgers CD, Raja A. Anatomy, Bony Pelvis and Lower Limb, Hamstring Muscle. [Updated 2022 Jan 29]. In: StatPearls [Internet]. Treasure Island (FL): StatPearls Publishing; 2022 Jan-. Available from: https://www.ncbi.nlm.nih.gov/books/NBK546688/
40. *SAM.gov*. (2022, March 11). SAM.gov. Retrieved October 24, 2022, from https://sam.gov/opp/35f25e1d7d254dc3a83ba358fc5d4370/view
41. Shah A, Bordoni B. Anatomy, Bony Pelvis and Lower Limb, Gluteus Medius Muscle. [Updated 2022 Jan 25]. In: StatPearls [Internet]. Treasure Island (FL): StatPearls Publishing; 2022 Jan-. Available from: https://www.ncbi.nlm.nih.gov/books/NBK557509/
42. Shankland, Stephen. "Brace Yourself: SuitX Industrial Exoskeletons Amplify Human Strength." CNET, CNET, 12 May 2018, https://www.cnet.com/science/suitx-industrial-exoskeletons-amplify-human-strength/.
43. UPMC HealthBeat. (2019, June 9). When is a backpack too heavy? UPMC HealthBeat. Retrieved September 24, 2022, from https://share.upmc.com/2017/06/backpacks-and-back-pain/
44. "Uprise® Passive Load-Bearing Exoskeleton." Mawashi Science & Technology - UPRISE*® Tactical Exoskeleton, Mawashi, 2020, https://mawashi.net/en/uprise-tactical-exoskeleton.
45. *Uprise® Passive Load-Bearing Exoskeleton*. (n.d.). Mawashi. Retrieved September 15, 2022, from https://mawashi.net/en/uprise-tactical-exoskeleton.
46. US Army Basic. (2016, October 21). Army height and weight standards for 2022. US Army Basic. Retrieved September 25, 2022, from https://usarmybasic.com/army-physical-fitness/army-height-weight-standards
47. Wang, Tianshuo, et al. "Design and Control of a Series–Parallel Elastic Actuator for a Weight-Bearing Exoskeleton Robot." Sensors., vol. 22, no. 3, 2022, p. 1055., https://doi.org/10.3390/s22031055.
48. Waterman, J., Hersum, A., Chapins, Z., Ferrua Elmudesi, R., & Habboosh, D. (2022). Autonomous Exoskeleton for Paraplegic Assistance. : Worcester Polytechnic Institute.
49. Watson, Bree. "Onyx Exoskeleton: An inside Look at Lockheed Martin's Wearable Robot." Pegasus Magazine, University of Central Florida, 30 Mar. 2020, https://www.ucf.edu/pegasus/power-move-onyx-exoskeleton/.
50. Watson, B. (2019). *Onyx Exoskeleton*. University of Central Florida. Retrieved September 2022, from https://www.ucf.edu/pegasus/power-move-onyx-exoskeleton/.

51. Wong M, Jardaly AH, Kiel J. Anatomy, Bony Pelvis and Lower Limb, Achilles Tendon. [Updated 2021 Aug 11]. In: StatPearls [Internet]. Treasure Island (FL): StatPearls Publishing; 2022 Jan-. Available from: https://www.ncbi.nlm.nih.gov/books/NBK499917/
52. *11B Infantryman*. (n.d.). Army National Guard. Retrieved October 24, 2022, from https://www.nationalguard.com/11b-infantryman
53. *92Y Unit Supply Specialist*. (n.d.). Army National Guard. Retrieved October 24, 2022, from https://www.nationalguard.com/92y-unit-supply-specialist